catalysts

MDPI

Review

Organic Chemistry and Synthesis Rely More and More upon Catalysts

Pierre Vogel [1,*] and Kendall N. Houk [2]

[1] Institute of Chemical Sciences and Engineering, Swiss Institute of Technology in Lausanne (EPFL), 1015 Lausanne, Switzerland
[2] Department of Chemistry and Biochemistry, University of California (UCLA), Los Angeles, CA 90095-1569, USA; houk@chem.ucla.edu
* Correspondence: pierre.vogel@epfl.ch; Tel.: +41-76-521-49-04

Abstract: A few months before the COVID-19 pandemic, Pierre Vogel and Kendall N. Houk published with a new textbook Wiley-VCH, "*Organic Chemistry: Theory, Reactivity, and Mechanisms in Modern Synthesis*", with a foreword from the late Roberts H. Grubbs. The book demonstrates how catalytic processes dominate all fields of modern organic chemistry and synthesis, and how invention combines thermodynamics, kinetics, spectroscopy, quantum mechanics, and thermochemical data libraries. Here, the authors present a few case studies that should be of interest to teachers, practitioners of organic and organometallic chemistry, and the engineers of molecules. The Vogel–Houk book is both textbook and reference manual; it provides a modern way to think about chemical reactivity and a powerful toolbox to inventors of new reactions and new procedures.

Keywords: catalyzed pericyclic reaction; π- and σ-complex; cycloaddition; diradicaloid; electron-releasing carbonyl group; ene-reaction; sigmatropic rearrangement; S_N2-displacement; thermochemistry; transition metal catalysts

Citation: Vogel, P.; Houk, K.N. Organic Chemistry and Synthesis Rely More and More upon Catalysts. *Catalysts* **2022**, *12*, 758. https://doi.org/10.3390/catal12070758

Academic Editor: Fabio Ragaini

Received: 1 June 2022
Accepted: 21 June 2022
Published: 8 July 2022

1. Introduction

Our planet and its people face new problems that require new solutions. Many of us are concerned by climate change, by the loss of biodiversity, by human population growth, by the ageing of people, by neurodegenerative diseases and cancer that are expanding, by the threat of new infectious diseases recently demonstrated so vividly, by the continuously increasing cost of medical care in general, by drinking water availability and its contamination, by air and ocean pollution, and by the degradation of the soil that nourishes us. These problems should not make us fall into a depressed funk. Most scientists are stimulated by these problems and can propose solutions that represent new opportunities for engineers, investors, and business. In the search for these solutions, new molecules and new devices are invented. The first industrial commodity produced by organic chemistry was Perkin's purple (mauveine) in 1856 [1–3]. The first synthetic drug was chloral hydrate ($Cl_3CCH(OH)_2$ introduced on the market in 1869, a compound prepared first by Liebig in 1832 (chlorination of ethanol) [4–6]. At that time, all dyestuffs and drugs were extracted from minerals, plants, and animals [7–9]. Only 300 organic compounds were known in 1800; the first edition of the Beilstein Handbook of Organic Chemistry described 20,000 organic compounds in 1882. Now, more than 80 million organic compounds are known. Nowadays, most dyestuffs are synthetic; most drugs are chemicals obtained through synthesis or are biologics derived from cell cultures [10,11]. At the end of the 19th century, most materials and commodities were made from minerals, plants, wood, animals, and metals. Today many of them are made out of polymers derived from fossil carbon. Sooner or later, engineers will find economical ways to obtain these commodities, and better ones, from left-overs of agriculture and forestry, and from urban waste [12]. The molecules and devices we need now are more and more sophisticated and must be invented at a faster and faster

pace. Scientists are exploring a larger and larger chemical space; they are engineers of the molecules who understand their structures from atoms, their dynamics (how they can be transformed), and the way they generate assemblies (macromolecules).

With increasing molecular complexity and sophistication of the procedures available, the study of chemistry represents a fantastic challenge. Scientists with experience and especially teachers are responsible for finding suitable models and explanations the beginners can apply as learning tools. This is done in a beautiful manner in the latest textbooks of organic chemistry [13–15] and for transition metal-catalyzed reactions in the book of Hartwig and colleagues [16]. In our textbook, we intend to complement these manuals critically, reviewing selected fundamental concepts and theories and using them to discuss a selection of reactions and processes that have been pivotal in the development of concepts and procedures, and which will hold even greater importance for sciences of matter in the future [17]. This textbook is a guide to quantitative and qualitative models that rely upon thermochemical data and kinetics, and shows how to grasp reactivity and molecular complexity such as asymmetric synthesis and catalysis. Here, we shall not summarize the whole book, but present a few study cases.

2. Invention Is Quicker if Physical Organic Chemistry Principles Are Integrated in Preparative Chemistry

The study of physical organic chemistry is a prerequisite for becoming a modern molecular scientist [18,19]. The main feature of physical organic chemistry is to associate chemical reactions that define chemical functions with quantitative measurements (equilibrium constants, heat of reaction, rate constants, isotopic effects). Chemical informatics estimate that 166.4 billion possible molecules can be made with up to 17 atoms of C, N, O, S, and halogens based on known or estimated stability of compounds and their possible reactions (known feasibility) [20]. When criteria of medicinal chemistry and pharmacokinetics are used to filter the above database, Reymond and co-workers estimate that about 10 million small molecules are potential drugs [21]. With the assistance of robots, these molecules can be obtained quickly and one can generate large libraries of new compounds, most of which are made by applying robust reactions (typically amide formation, Suzuki–Miyaura C–C-coupling, Buchwald–Hartwig nucleophilic aromatic substitutions, azide + alkyne cycloadditions) [22–25]. We think this is not optimal today; the chemical space exploration must add many less-common reactions, especially recently developed catalytic processes [26]. Moreover, reactions permitting access to enantio-pure compounds (asymmetric synthesis) must be developed and applied. This requires not only imitation of literature procedures, but the invention of new and better ones. Nature remains a source of inspiration; complicated bioactive compounds such as alkaloids, polyphenols, polyketides, peptides, nucleic acids, oligosaccharides, and glycoproteins, as well as their mimics, should be available through synthetic chemistry. Synthesis can produce analogs and eventually better drugs than those offered by nature. For that, knowledge of physical chemistry, physics, mechanics (when designing micro-reactors and automatic systems, for instance), quantum chemistry, and the application of artificial intelligence can be quite beneficial. Molecular scientists must have a profound understanding of chemical reactivity and must be able to predict whether a planned reaction is possible or not, and at what rate it will occur under the conditions chosen. For more than 100 years, successes of synthetic chemistry have been the result of trial and error and serendipity [27]. This has turned many talented students away from synthesis and from chemistry. Today, synthetic chemistry, and especially organic and organometallic chemistry in homogeneous systems, is a reliable science with reproducible procedures based on thermodynamics, kinetics, and availability of highly performing analytical tools. Scientists using all this knowledge and techniques have more productive and inventive intuition [28]. The relationships between molecule dynamics and energy (heat, light) are established on a quantitative basis. With the help of quantum mechanical calculations, one can invent models that can be applied to almost any reaction. Literature and data banks (e.g., NIST WebBook of Chemistry [29]) provide us

with quantitative and accurate thermodynamic data. The latter must be used to predict chemical reactivity (equilibrium constant and reaction rates) and the properties of the new compounds targeted. This is one of the messages that the Vogel–Houk book tries to pass to students, chemists, biochemists, and engineers. The domestication of fire one million years ago has permitted humans to continuously improve their quality of life. The treatment of matter with heat has created new objects and new knowledge (metallurgy, pottery, ceramics). The understanding of how matter and heat are interrelated is the basis of the sciences of matter. This should be kept in mind when teaching or/and applying chemistry, for instance.

Because the transformation of matter should not produce waste, atom economical reactions should be preferred to reactions producing co-products [30–32]. Catalytic processes should be chosen, as they save significant energy; furthermore, they should be run in inexpensive, non-toxic, and recoverable solvents, if any.

Amide formation is one of the most important reaction in cells and in the laboratory. The direct amidification of carboxylic acids by amines requires the elimination of water [33]. New catalysts have been invented that achieve direct amidification of carboxylic acids with amines in an aqueous solvent (DMSO, 70 °C) [34].

$$CH_3COOH + MeNH_2 \rightleftarrows CH_3CONHMe + H_2O \quad (1)$$

Thermochemical data for Equilibrium (1) in the gas phase tells us that this direct amidification is exothermic, with $\Delta_r H^\circ(1) = -8 \pm 1.5$ kcal mol^{-1}. Gas phase experimental entropies are not available for Me_2NH and CH_3CONMe_2. The entropy variation $\Delta_r S^\circ(1)$ of Equilibrium (1) under 1 atmosphere and at 25 °C can be estimated from the variation of translation entropies [35], which depend on the molecular weights of reactants and products, according to Equation (2) for equilibrium **A** + **B** $\rightleftarrows$ **P** + **Q**:

$$\Delta_r S^\circ(\mathbf{A} + \mathbf{B} \rightleftarrows \mathbf{P} + \mathbf{Q}) \cong \Delta_r S^\circ{}_{trans} = 1.5\ R\ln(M_P \cdot M_Q / M_A \cdot M_B) \quad (2)$$

For Equilibrium (1) in the gas phase, $\Delta_r S^\circ(1) \cong -1$ eu (entropy unit = cal mol^{-1} K^{-1}). This gives an entropy cost of $-T\Delta S_r^\circ \cong 300$ cal mol^{-1} = 0.3 kcal mol^{-1} at 25 °C. This indicates that the reaction must be exergonic ($K^{298K}(1) > 1$): $\Delta_r G^\circ = \Delta_r H^\circ - T\Delta S_r^\circ \cong -7.7 \pm 1.5$ kcal mol^{-1} at room temperature. In solution, this value will be affected by differential solvation effects, and, when using larger carboxylic acids than acetic acid and different amines than methyl amine, the entropy variation will be more negative (e.g., for a carboxylic acid and an amine having both a molecular weight of 200, one obtains with relationship (2) $\Delta_r S^\circ \cong -5$ eu, and an entropy cost $-T\Delta S_r^\circ \cong 1.5$ kcal mol^{-1}). Thermochemical data for model Equilibrium (1) in the gas phase should encourage chemists to look for more catalysts that can induce the direct formation of amides at room temperature without a co-solvent such as DMSO, or with a co-solvent that can be recovered more readily, as well as for carboxylic acids and amines that contains other functions (e.g., ketone, aldehyde, ester, etc.). We hope that this example will convince chemists, biochemists, and engineers to use thermochemical data available for compounds in the gas phase, even though the planned reaction must be run in solution and at a temperature different than 25 °C.

3. Thermochemical Data Establish Fundamental Concepts of Reactivity

Under thermodynamic control, substitutions of alkyl halides (e.g., Equilibrium (3), Pr = prop-1-yl) and of alkenyl halides (e.g., Equilibrium (4), vinyl = CH_2=CH) by other halides generally favor the formation of H-F in the gas phase:

$$Pr\text{-}F + HBr \rightleftarrows Pr\text{-}Br + H\text{-}F \quad (3)$$

$$vinyl\text{-}F + HBr \rightleftarrows vinyl\text{-}Br + H\text{-}F \quad (4)$$

In contrast, Equilibria (5) that exchange the fluoride of acetyl fluoride (Ac-F = CH_3CO-F) with chloride, bromide, or iodide with the corresponding hydrogen halide H-X disfavor

the formation of H-F, meaning that fluorine prefers to be bonded to an acyl carbon atom rather than to a hydrogen atom. In contrast, equilibria of acetyl chloride (Ac-Cl) with the corresponding bromide and iodide are nearly thermoneutral in the gas phase.

$$\text{Ac-F} + \text{H-X} \rightleftarrows \text{Ac-X} + \text{H-F} \quad (5)$$

$$\Delta_r H^o(5) = 4.6\ (X = Cl),\ 4.0\ (X = Br),\ 4.0\ (X = I)\ \text{kcal mol}^{-1}$$

Why does fluorine prefer the left side (C center instead of the H atom) of Equilibria (5)? Donation of the non-bonding electrons of the oxygen atom of the carbonyl group stabilizes the ionic form of the acetyl-halide bond. This negative hyperconjugation effect (n(C=O:)/σ* interaction) involves the interaction of the non-bonding or lone pair, orbitals n(CO:) of the carbonyl group, and the anti-bonding, empty orbital σ*(C-F) of the C-F bond. This interaction is not possible in alkyl, alkenyl, and hydrogen halides, which do not possess lone pair electrons. Of all acyl halides, this hyperconjugative interaction is strongest in acyl fluorides, where the difference in electronegativity between carbon and fluorine is larger than in the other acyl halides. Because of the large electronegativity difference between F and C, σ*(C-F) is the best σ-acceptor of all C-X bonds. Furthermore, the conjugation n(X:)/π*(C=O) (donation from the non-bonded electron pairs of X: to the carbonyl double bond), which stabilizes the carbonyl compound, is the weakest for X=F, and strongest for amino groups (Figure 1). The infrared carbonyl stretching frequencies of acyl derivatives ($\nu_{C=O}$) increase with the C=O bond strength, as shown below.

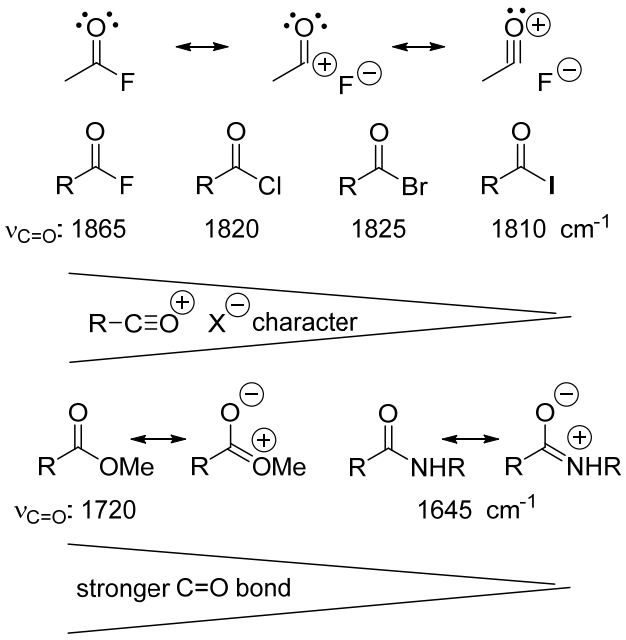

Figure 1. Hyperconjugation in acyl halides (donation from the carbonyl group n(CO:) non-bonded electron-pairs to the σ(C-X) bond) competes with the n(X:)/π(C=O) conjugation. This competition exists also in carboxylic esters and carboxamides. Reprinted with permission from Ref. [17]. Copyright 2019 Wiley.

The thermochemical data presented above demonstrate that a carbonyl group is a π-withdrawing and a σ-donating group [36–38]. This explains the regioselectivity of the electrophilic additions (6) to the alkene moiety of bicyclo[2.2.1]hept-5-en-2-one (**1**) to be the opposite of those of its synthetic precursors, the corresponding cyanoacetate (**4**) (reactions (7), Scheme 1) [39–41]. Quantum mechanical calculations find that the 6-oxobicyclo[2.2.1]hept-2-yl (**2**, E=H) cation is much more stable than its 5-oxo isomer [42,43]. The former carbocation is stabilized by n(CO)/σ(C(1)-C(6))/π(C(6)) hyperconjugation, what is not possible in the latter isomer. This type of interaction allows keto [44] and ester

groups [45] to migrate more quickly in Wagner–Meerwein and pinacolic rearrangements than alkyl and phenyl groups.

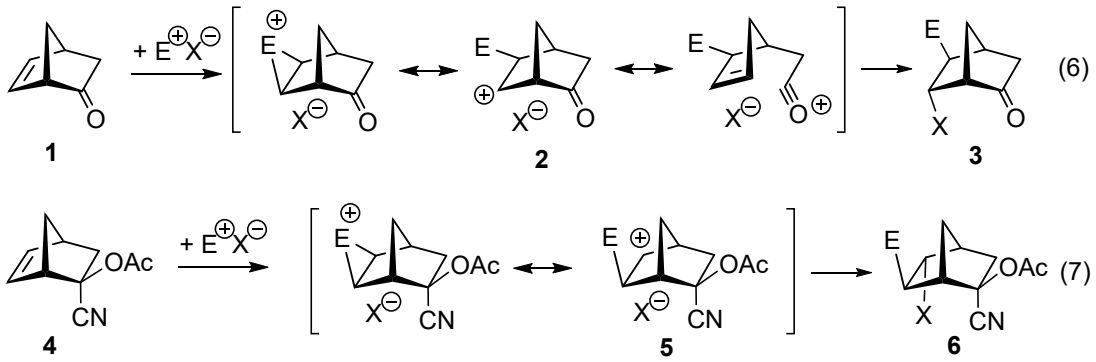

Scheme 1. Homoconjugated carbonyl group can be electron-releasing. Norborn-5-en-2-one (**1**) adds to electrophiles E-X giving the corresponding adducts **3** with high stereo- and regioselectivity arising from the quenching of cationic intermediates **2** by the nucleophiles X^-. 2-Cyanonorborn-5-en-2-yl acetate (**4**) adds to electrophiles E-X with opposite regioselectivity giving the corresponding adducts **6** arising from the quenching of cationic intermediate **5** by the nucleophiles X^-. In cationic intermediates **2** the positively charged center C(6) is homoconjugated with the carbonyl group whereas in cationic intermediates **5** the positive charge prefers to reside on C(5), away from the two electron-withdrawing substituents CN and AcO.

Carbon monoxide (C=O) has a dipole moment that places a partial negative charge on its carbon atom [46,47]. In contrast, carbon dioxide (O=C=O) has partial negative charges on its two oxygen atoms and a partial positive charge on its carbon atom. Carbon monoxide is in fact an electron-rich carbene because of the electron donation by the non-bonding electron of its oxygen atom. In carbonylmetal complexes, CO is a σ-donor and a π-attractor.

$$M{=}C{=}O \leftrightarrow M^{(-)}\text{-}C{\equiv}O^{(+)}$$

4. Mnemonic Devices Are Very Useful to Learn Chemistry, but They Must Be Applied Critically

We now discuss Markovnikov's rule about the orientation of the additions of H-X to alkenes. The rule states that when water, a carboxylic acid, or a hydrogen halide adds to an unsymmetrical alkene, the hydrogen atom joins the carbon atom bearing the largest number of hydrogen atoms and the nucleophile (X) bonds to the vicinal center that is more substituted. The classic explanation invokes a two-step mechanism in which the proton adds first to the alkene forming a carbenium ion intermediate in the rate determining step, which is then quenched by the nucleophile irreversibly. This hypothesis implies kinetic control (the rate of the two competing regioselective additions are different and the major regioisomer results from the fastest reaction). The stability sequence for alkyl cations is tertiary > secondary > primary [48–50]. However, in addition, in the cases where R-X are alcohols, amines, thiols, and alkyl halides, secondary derivatives are more stable than their primary isomers (see Equilibria (8)). Similarly, tertiary systems are more stable than their secondary isomers [51]. The formulation of Markovnikov's rule as a kinetic control is not always valid [52–55]. Additions to alkenes are exothermic but have negative entropies (condensations) that can cause the reactions to be reversible (with standard Gibbs energy variation $\Delta_r G^T = \pm 1$ kcal/mol). For example, additions of water to unstrained alkenes in the gas phase are exothermic by ca. −12 kcal/mol, a value very similar to the entropy cost of the addition at 25 °C. For instance, in the gas phase, the standard heat of reaction $\Delta_r H^\circ$(2-methylpropene + $H_2O \rightleftarrows$ *t*-butanol) ≅ −12.6 kcal/mol, and the standard entropy variation of the equilibrium $\Delta_r S^\circ$(2-methylpropene + $H_2O \rightleftarrows$ *t*-butanol) ≅ −37 eu; at 25 °C, the entropy cost $-T\Delta_r S^\circ$ amounts to $-298\cdot(-37$ cal mol^{-1}K$^{-1}) \cong 11.0$ kcal mol^{-1} [29,56].

Thus, one predicts that the regioselectivity of the additions of water, alcohols, and carboxylic acids to acyclic alkenes might be thermodynamically rather than kinetically controlled above 25 °C. As shown with Equilibria (8) in the gas phase, the linear adducts are less stable than their "branched" isomers. Additions of HX to terminal alkenes or 1,2-dialkylethylenes avoid the generation of secondary carbenium intermediates and follow other mechanisms that do not involve carbenium ion intermediates. The reverse reactions, that is, eliminations, also may follow concerted mechanisms avoiding carbenium ion intermediates. Even for such reactions, Markovnikov's rule is generally followed. This is because of the Dimroth principle, which was enunciated in 1933 [57]. If one or a set of reactants can undergo two competitive one-step reactions that follow the same mechanism and produce two different isomers, the favored product under conditions of kinetic control is the most stable one. The energy barrier is the lowest for the most exothermic reaction (Bell–Evans–Polanyi theory established in 1936–1938 for radical exchange reactions such as R-X + $Y^{\bullet}$ → $R^{\bullet}$ + X-Y, and proton transfers: $\Delta^{\ddagger}H = \alpha\Delta_r H + \beta$) [58,59]. Deviations to this principle are observed when differential steric factors and solvation effects affect the reactions.

$$\text{Prop-1-yl-X} \rightleftarrows \text{Prop-2-yl-X} \quad (8)$$

X =	Me	Et	*n*-Pr	OH	SH	NH_2	F	Cl	Br	I
$\Delta_r H°$(8):	−2.0	−1.6	−1.8	−4.2	−4.0	−3.2	−1.8	−3.1	−3.0	−2.4 kcal mol^{-1}

Mnemonic tools such as the Markovnikov's rule and the ever-popular arrow-pushing are very useful when one learns chemistry [60]. At some point, we need to remember how they have been constructed and on what measurements they are based upon. Scientists should not be afraid to be critical of the models proposed to them and should ask for more experimental proofs.

5. Models Must Be Based on Measurements and Thermochemical Data

We next discuss the mechanisms of some pericyclic reactions. Among them, cycloadditions, cheletropic additions, and ene-reactions all permit the construction of C-C and C-hetero bonds in an atom economical fashion, sometimes with high chemo-, regio-, stereo-, and enantioselectivity. Isomerizations such as electrocyclic ring opening or closing reactions and sigmatropic rearrangements are also very interesting synthetic tools and will continue to play an important role in synthesis. Most pericyclic reactions tolerate a large variety of substituents and permit access to a large molecular diversity. Furthermore, these reactions can be catalyzed and run under very smooth conditions, saving energy. Before 1965, concerted pericyclic processes were called "no-mechanism reactions" to imply that there are no detectable intermediates and everything happens in one step. Since then, the study of their mechanisms has revealed many subtleties and has contributed enormously to our understanding of chemical reactivity. Depending upon the nature of the reactants (type of substituents, number of substituents, etc.) and reaction conditions (temperature, solvent, presence of additives and of catalysts), the pericyclic reactions may not follow concerted, one-step mechanisms, but can be multi-step processes.

The Woodward–Hoffmann rules explain the stereoselectivity of concerted pericyclic reactions [61]. The rules and other related theories such as the Longuet–Higgins correlation of electronic configurations between reactants and products rely upon symmetry in the transition structures [62]. Perfectly symmetrical transition structures are very rare, especially when non-symmetrical reactants are engaged (as demonstrated by kinetic isotopic effects). The activation enthalpy ($\Delta^{\ddagger}H$) of a concerted reaction is the sum of repulsive steric effects and skeletal distortion energies, minus stabilization energies resulting from stabilizing orbitals interactions in the transition state [63]. The FMO theory applied to transition structures of pericyclic reactions also predicts their stereochemistry, as well as their aromatic character [64,65] (Evans' rule) [66]. FMO theory provides estimates of substituent and additive effects on the rate and the chemo-, regio-, and stereoselectivity of the reactions without requiring symmetrical transition structures [67]. Another approach takes advantage of the fact that non-symmetrical transition structures of pericyclic reactions are

diradicaloids, i.e., species with very narrow HOMO–LUMO gaps, or in valence bond terminology, diradical ↔ zwitterion species. Thus, without having to calculate molecular orbitals, by using just thermochemical data (homolytical bond dissociation enthalpies: $DH^\circ(R^\bullet/H^\bullet)$ or $DH^\circ(R^\bullet/X^\bullet)$), the substituent effect on the relative stability of radicals, cations and anions, ionization energies ($IE(R^\bullet)$ [68], and electron affinities of radicals ($-EA(R^\bullet)$) [69] can be used to predict relative rates and chemo-, regio-, and stereoselectivities of concerted, one-step pericyclic reactions. The diradicaloid model, advocated by Dewar for Diels–Alder reactions [70,71], is simple because it is based on thermochemical data (measurements) and it can be applied to catalyzed pericyclic reactions.

For the cyclodimerization of ethylene into cyclobutane (reaction (9), gas phase, 25 °C, 1 atm.), one estimates the temperature at which cyclobutane equilibrates with ethylene. The equilibrium constant $K^T(9) = 1$ ($\Delta_r G^\circ = \Delta_r H^\circ - T\Delta_r S^\circ = 0$) is realized at a relatively low temperature, as given by $\Delta_r H^\circ/\Delta_r S^\circ \approx 18{,}400/41.6 \approx 442$ K = 169 °C. Above this temperature, the cyclodimerization is endergonic ($K^T < 1$). The cycloreversion of cyclobutane into ethylene occurs between 350 and 450 °C with a measured barrier $\Delta^\ddagger H = 61.1$ kcal mol^{-1}. One calculates $\Delta_f H^\circ$ (tetramethylene diradical) = $\Delta_f H^\circ$ (cyclobutane) + DH° ($Et^\bullet/Et^\bullet$) – ring strain of cyclobutane = 6.6 + 86.0 − 26.5 = 66.1 kcal mol^{-1}. This gives an enthalpy difference $\Delta_r H^\circ$(cyclobutane ⇄ tetramethylene diradical) = 66.1 − 6.6 = 59.5 kcal mol^{-1}. With a measured barrier $\Delta^\ddagger H$(cyclobutane → 2 ethylene) = 61.1 kcal mol^{-1}, the thermochemical data support the hypothesis of a diradical mechanism for the cycloreversion (9), which has been demonstrated through femtochemistry by Zewail and co-workers [72]. The reaction is not concerted or pericyclic; there is no assistance between the σ-bond breaking and π-bond forming processes (Scheme 2). The thermally "allowed" concerted [π^2s + π^2a] cycloreversion is not followed, since it involves too severe distortions of cyclobutane to reach the twisted transition structures predicted by the Longuet–Higgins theory and the Woodward–Hoffmann rules. The entropy of activation $\Delta^\ddagger S$ of this condensation is that of the reaction $\Delta_r S^\circ$ corrected for the three free rotations about the three single C-C bonds of the 1,4-diradical (3 times 5 eu). This leads to the estimated $\Delta^\ddagger S = -41.6 + 15 \approx -27$ eu. One obtains finally the Eyring activation free enthalpy $\Delta^\ddagger G = \Delta^\ddagger H - T\Delta^\ddagger S = 41 - 442\cdot(-0.027) \approx 53$ kcal mol^{-1} (with $\Delta^\ddagger H$ = Eyring activation enthalpy). Using equation $\ln k = -\Delta^\ddagger G/RT + \ln T + 23.76 = -53{,}000/1.987\cdot 442 + \ln(442) + 23.76 \approx -30.7$, one obtains a rate constant $k(9) \approx 4.6 \times 10^{-14}$ dm^3 mol^{-1} s^{-1}, or a half-life (time for 50 % conversion) $\tau_{\frac{1}{2}} = 1/k(9)$ [initial concentration of ethylene = 1] ≈ 682,400 years! This reaction is too slow to be observed at 442 K.

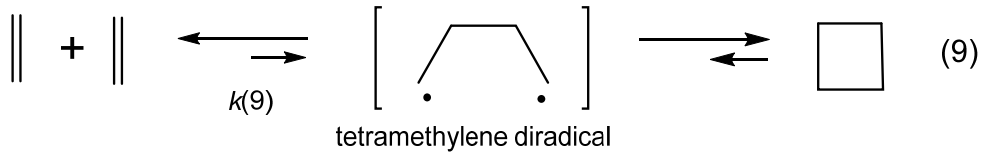

Scheme 2. Many (2 + 2)-cycloadditions and (2 + 2)-cycloreversions involve 1,4-diradical intermediates.

If one considers the substituent effects on the relative stability of radicals, one can predict the relative rate and the regioselectivity of all (2 + 2)-cycloadditions of alkenes. Thermochemical analysis analogous to that given for the cyclodimerization (9) of ethylene into cyclobutane suggests that the octa-1,7-diene-3,6-diyl diradical is also an intermediate of the (2 + 2)-cyclodimerization of butadiene. When the alkenes are substituted with polar groups, their cycloadditions are solvent dependent because zwitterions can be formed in place of diradicals.

6. Diradicaloids Are Transition Structures of Concerted Cycloadditions

Figure 2 represents the possible paths of a Diels Alder reaction. For the same orientation (regioselectivity), there are three limiting mechanisms; two of them involve the formation of (*Z*)-hex-5-en-1,4-diyl diradicals, and the third one corresponds to the synchronous one-step reaction, as implied by the Woodward–Hoffmann rules. Between these

extremes are the concerted but two-stage mechanism proposed in 1959 by Woodward and Katz [73]. For the retro-Diels–Alder reaction of norbornene into cyclopentadiene and ethylene, Zewail and co-workers proposed from their femtosecond real-time studies that both concerted and non-concerted trajectories are possible; however, they decomposed norbornene by an intense laser pulse and generated the diradical by a photochemical process [74]. Were (*E*)-hex-5-en-1,4-diyl diradicals to be formed, they could not cyclize, but would induce polymerization of the cycloaddends, as already discussed by Littmann in 1936 [75]. Polymerization often accompanies cycloadditions of relatively unreactive dienes unless a radical scavenging agent is added to the reaction mixture. In between the three limiting mechanisms defined above, a spectrum of non-synchronous one-step mechanisms are generally thought to occur, as supported on the basis of kinetic isotope effects [76].

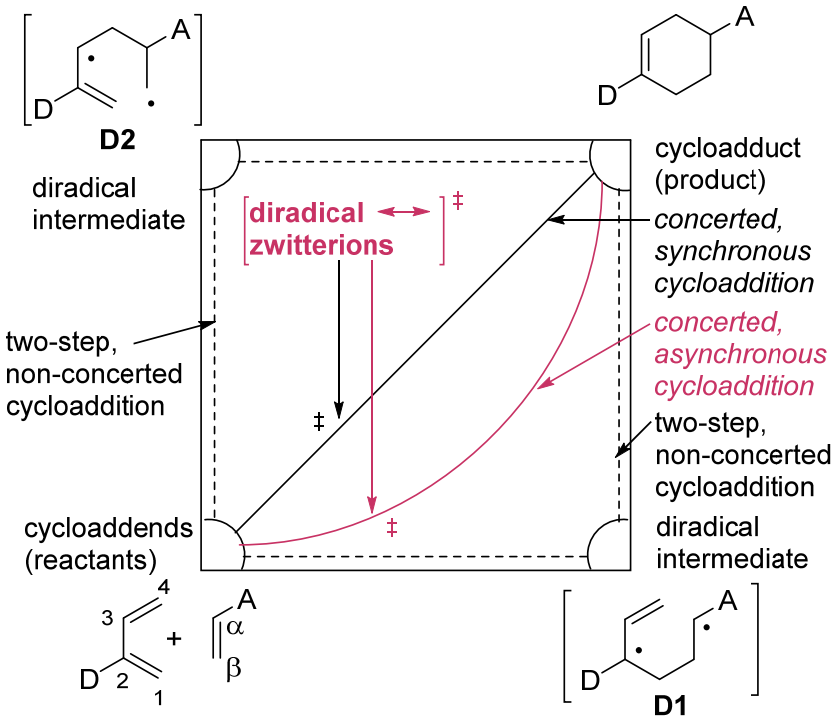

Figure 2. Spectrum of mechanisms for the Diels already Alder reaction. In polar medium and for polar substituents, the diradical intermediates **D1** and **D2** can be zwitterions. ‡ for transition states.

Thermochemical data tell us that the preferred diradical intermediate is the one for which the substituents stabilize the radicals the best, and this implies, as a rule, that this diradical results from combining the least substituted centers of the diene and dienophile. In other words, the most stable isomeric diradical intermediate is the one that has generated the strongest bond between the two reactants (for instance **D1** or **D1'**, Figure 3). Since many Diels−Alder reactions have measured activation enthalpies $\Delta^{\ddagger}H$ that are lower than the enthalpy difference $\Delta_{r}H^{\circ}$ between the diradical and the cycloaddends, the difference $\Delta_{r}H^{\circ} - \Delta^{\ddagger}H$ can be taken as Doering's energy of concert (Figure 3). The transition state of such reactions can be readily described in terms of frontier molecular orbital interaction theory [77,78]. An alternative valence-bond representation is that transition structures can be represented by diradicaloids, i.e., diradicals that exchange electron between the two radical entities. Within the valence bond theory, this electron exchange can be represented by a (Z)-diradical and one or two zwitterions, as shown in Figure 3 with **D1** ↔ **Z1** ↔ **Z2**.

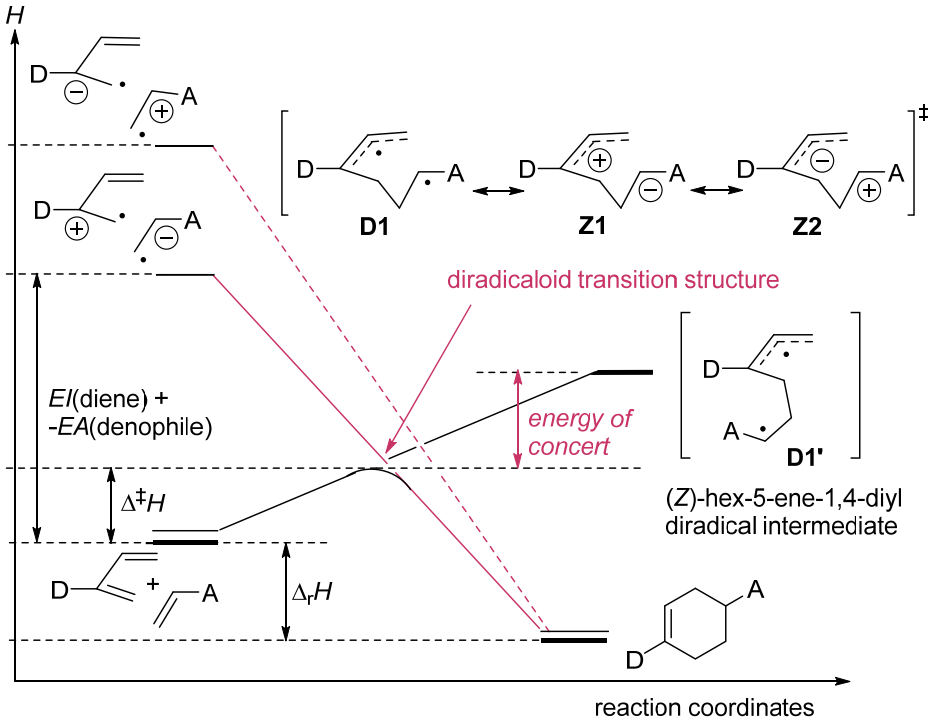

Figure 3. The valence-bond diradicaloid model for transition states of concerted Diels–Alder reactions. The lower is the sum *EI*(diene) + (−*EA*(dienophile)), or *EI*(dienophile) + (−*EA*(diene)); the faster is the cycloaddition; the higher is the degree of concert.

The diradicaloid model explains the chemo-, regio-, and stereoselectivity (e.g., endo rule of the Diels–Alder reactions) of all cycloadditions and cheletropic additions. If one of the substituents A or D can be coordinated selectively to an additive, a catalytical effect can be observed, which is explained also by the diradicaloid model.

7. Diradicaloid Transition Structures of Concerted Sigmatropic Rearrangements

Sigmatropic rearrangements and especially the (3,3)-sigmatropic rearrangements such the 3,4-diaza-Cope rearrangement in the Fischer's indole synthesis, the Claisen rearrangements and its various variants, the aza-Claisen, the Overman, and the Cope rearrangements have played an important role in synthesis, and will continue to do so. Here, also one considers a spectrum of mechanisms (Figure 4) in which there are two limiting paths involving diradical intermediates, and in between these two limits, concerted one-step mechanisms. One limiting mechanism is dissociation with the formation of two allyl radicals **7** + **8**; the other is the associative formation of cyclohexa-1,4-diyl diradical intermediate of type **D3** (Grob's hypothesis).

Gajewski and Conrad mapped out the positions of transition states on such diagrams through their measurements of secondary deuterium kinetic isotope effects and comparisons to equilibrium isotope effects [79]. In the concerted one-step mechanisms, the bond forming process assists the bond breaking process. Their transition states can be represented by transition structures belonging to two types of diradicaloids (Figure 5). The two allyl radicals **7** + **8** exchange an electron, forming ion-pairs **IP1** or/and **IP2**. On its side, diradical **D3** is stabilized by electron-exchange leading to zwitterions **Z3** or/and **Z4**. Substituent effects on the relative stability of radicals, cations, and anions allow one to predict the reactivity of these concerted reactions. This model explains substituent effects on rates and the accelerating effects of catalysts. For instance, any additive that can stabilize one or the other of the charge-transferred limiting structures will catalyze the (3,3)-sigmatropic rearrangement.

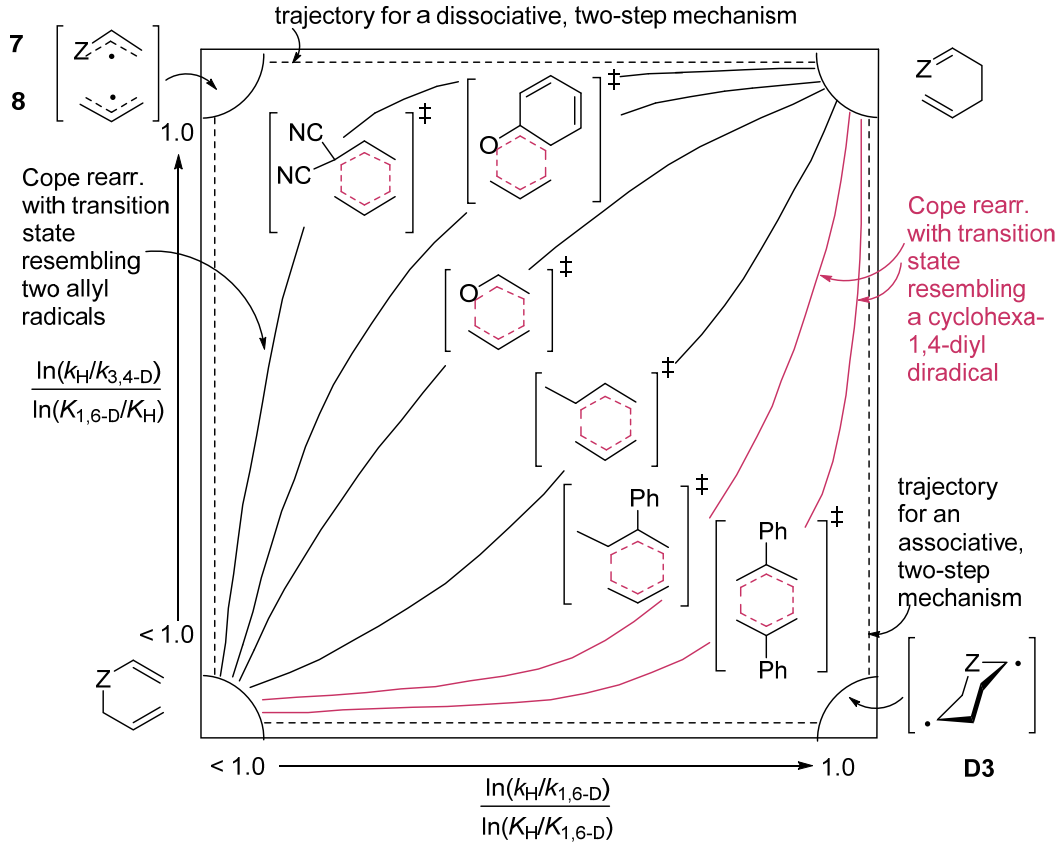

Figure 4. More O'Ferrall–Jencks diagram for Cope and Claisen rearrangements. The horizontal coordinate represents the shortening of the C(1)-C(6) distance; the vertical coordinate represents the lengthening of the σ(C(3)-C(4)) bond; the enthalpy is perpendicular to the plane made by the two former coordinates. The position of the transition states (‡) in this diagram are deduced according to Gajewski from the comparison of kinetic and equilibrium deuterium isotopic effects.

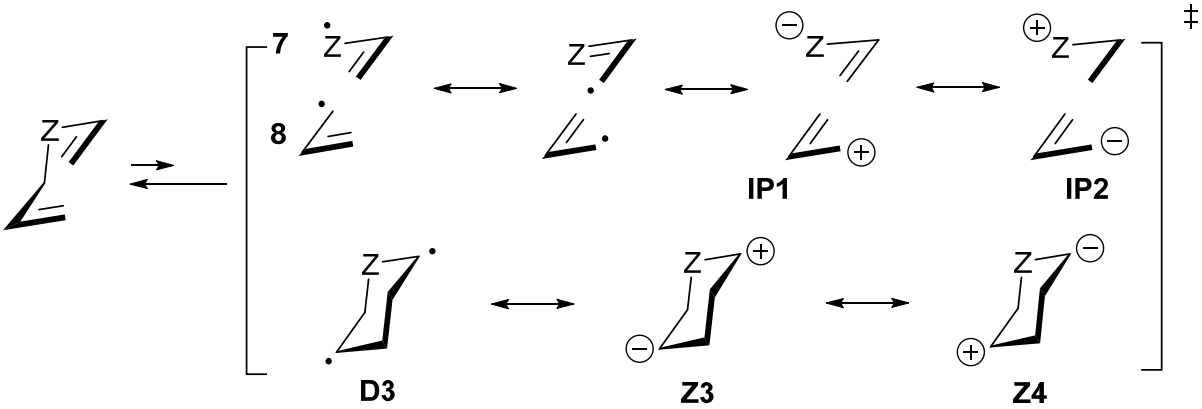

Figure 5. Diradicaloid model for the variable transition states of the (3,3)-sigmatropic rearrangements.

8. Diradicaloid Transition Structures in Concerted Ene-Reactions and Related Processes

The Alder−ene reaction is the thermal reaction of two alkenes that are condensed into another alkene with the formation of a new σ(C-C) bond and the transfer of a hydrogen atom between them. A large number of analogous reactions are known for heteroatoms containing unsaturated reactants, such as the aldol reaction (10) and the carbonyl-ene reaction (11) (Figure 6). In the absence of Lewis or Brønsted acid, the transition structure of the enol aldol condensation can be represented by a diradicaloid (1,4-diradical ↔ 1,4-zwitterion) of type **D4** ↔ **Z5** if it follows a concerted one-step mechanism (Figure 6, reaction

(10)). The role of the acid catalyst A is to stabilize the zwitterionic limiting structure **Z5** by equilibrating with zwitterion **Z5′**. As a consequence, the reaction may follow a multi-step mechanism in which **Z5′** is one reaction intermediate that can adopt quasi-cyclic or acyclic conformations. Similar diradicaloid models (**D5** ↔ **Z6**) can be considered for metalla-carbonyl-ene reactions promoted by a Lewis acid (Figure 6, reaction (11)). Very electrophilic ketones such as hexafluoroacetone react with allylsilanes without catalyst [80]. The Hosomi–Sakurai reaction promoted by $TiCl_4$ (Figure 6, reaction (11)) is not only regiospecific, but also stereospecifically *anti* with respect to the silyl group, which leads to the formation of a (*E*)-homoallylic alcohol [80–82]. ((*E*)-crotyl)trimethylsilane and ((*E*)-cinnamyl)trimethylsilane react with aldehydes in the presence of $TiCl_4$ to give homoallyl alcohols with over 93% *syn*-selectivity (Figure 6, reactions (12) and (13)). Lower *syn*-selectivity is observed for the reactions of (*Z*)-crotylsilanes [83,84]. The stereoselectivity is generally accepted to be determined by chair-like six-membered ("closed") transition states [85–90].

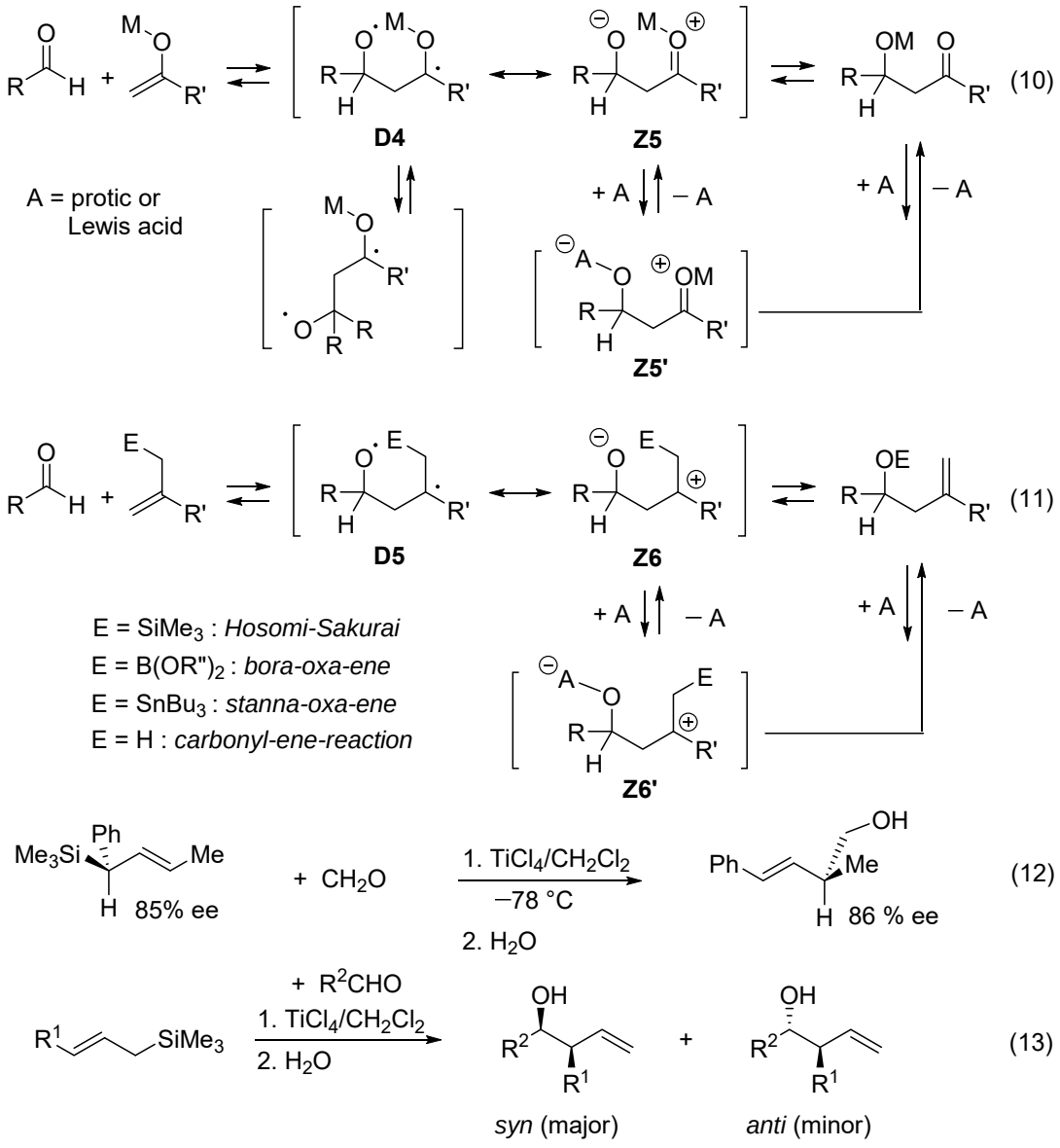

Figure 6. The diradicaloid model illustrated with Equilibria (10) and (11) permits to explain the catalytic effect of added protic or Lewis acids (A) to enolate aldol condensations, to metalla-carbonyl-ene reactions, and the carbonyl-ene-reaction.

9. Valence Bond Theory Can Be Used to Explain Structural and Medium Effects on the Rates of Displacement Reactions

The diradicaloid model is not limited to the transition structures of concerted pericyclic reactions. Concerted displacement reactions (14) are quite important in synthesis.

$$R\text{-}X + Y{:}^{-}/M^{+} \rightleftarrows R\text{-}Y + X{:}^{-}/M^{+} \quad (14)$$

Shaik and Pross, as well as others, have described the S_N2 reaction transition states in terms of valence bond theory [91–98]. The transition structure of a S_N2 reaction (Figure 7) engaging a negatively charged nucleophile can be represented by the limiting structures:

$$[Y{:}^{-}/R^{\bullet}/X^{\bullet} \leftrightarrow Y{:}^{-}/R^{+}/X{:}^{-} \leftrightarrow Y^{\bullet}/R^{\bullet}/X{:}^{-} \leftrightarrow Y^{\bullet}/R{:}^{-}/X^{\bullet}]^{\ddagger}.$$

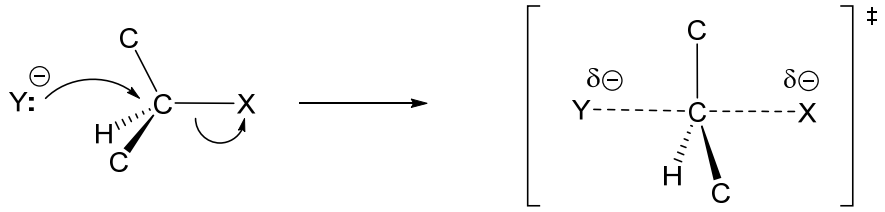

Figure 7. Classical representation of the transition state of a S_N2 displacement reaction.

This representation allows one to predict that the weaker the R-X bond ($DH^{\circ}(R^{\bullet}/X^{\bullet})$ = $\Delta_f H^{\circ}(R^{\bullet})$ + $\Delta_f H^{\circ}(X^{\bullet})$ - $\Delta_f H^{\circ}$(R-X), $\Delta_f H^{\circ}$ = standard heat of formation); the faster the nucleophilic displacement. Furthermore, the higher the stability of cation R^+ and of nucleofugal group $X{:}^{-}$, or/and the higher the stability of the carbanion $R{:}^{-}$ the faster the reaction is. Nucleophilicity of $Y{:}^{-}$ depends on how much the anion is dissociated from its counter-ion M^+, and this depends upon the medium polarity and/or catalyst that interact specifically with M^+. The lower the ionization energy ($EI(Y{:}^{-})$) of the nucleophile $Y{:}^{-}$, the faster the displacement reaction is. The higher the electron affinity ($-EA$(R-X)) of the electrophile R-X, the faster the reaction is. Thermochemical data such as ionization energies and electron affinities permit one to evaluate the power of the pushing effect of the arrow associated with the attack of the electrophile by the nucleophile, and of the power of the pulling effect of the arrow associated with the departure of the nucleofugal group $X{:}^{-}$. Additives that can combine with the nucleofugal group X (and not with the nucleophile Y) are catalysts of the displacement reaction.

10. Hydrocarbation of Unsaturated Compounds by R-H Reagents Do Not Produce Waste

Classically, for the formation of single C-C bonds, chemists have relied upon displacement reactions by matching a nucleophile with an electrophile (e.g., Nu-H + R-X + base → Nu-R + base-H^+/X^-, or Nu-metal + R-X → Nu-R + $metal^+/X^-$; R = alkyl, alkenyl, aryl, heteroaryl, alkynyl) [99] and on electrophilic substitutions (Ar-H + E-X ⇄ Ar-E + HX; e.g.,: Friedel–Crafts alkylation and acylation) [100]. Catalyzed or photo-catalyzed free-radical additions to C-C multiple bond are applied more and more in fine organic synthesis, not only to generate polymers (e.g., R-X (X= I, Br) + BCH=CHA → R-CH(B)-CH(X)-A) [101–106]. Aldehyde and ketone olefinations are also powerful methods to create double C=C bonds. All these reactions are not atom economical, as they produce co-products. The same can be said for the very much used additions of organometallic reagents to unsaturated systems (Nu-metal + A=E ⇄ Nu-A-E-metal, with A, E = carbon or heteroelement; = is a double or triple bond) [107]. Direct additions (15) of R-H to unsaturated compounds are more atom economical [108,109]. One-step concerted [π^2s+σ^2s]-cycloadditions are predicted to be difficult reactions (symmetry forbidden, small LUMO/HOMO overlap, and large energy gaps between these reactant MO's). Conformational strain required for the theo-

retically allowed concerted [π^2a+σ^2s]- or [π^2s+σ^2a]-cycloadditions renders these one-step reactions impossible.

$$\text{R-H + X=Y} \rightleftarrows \text{R-X-Y-H} \quad (15)$$

Many of them are base-catalyzed and involve the conjugate bases R^- of R-H as intermediate. Examples are the aldol (e.g., $R^1CHO + R^2CH_2COR^3 \rightleftarrows R^1CH(OH)\text{-}CH(R^2)\text{–}COR^3$) and the Claisen condensation (e.g., $R^1CH_2COOR^2 + R^3CHO \rightleftarrows R^1CH(COOR^2)\text{–}CH(OH)R^3$), the Henry reaction (e.g., $R^1CH_2NO_2 + R^2CHO \rightleftarrows R^1CH(NO_2)\text{-}CH(OH)R^2$), and the Michael addition (e.g., $R^1CH_2COR^2 + CH_2{=}CHCOR^3 \rightarrow R^1CH(COR^2)\text{-}CH_2\text{–}CH_2COR^3$) [110]. Under acidic conditions, the most common reactions are the Mannich reaction (e.g., $R^1COCH_3 + CH_2O + R_2NH \rightarrow R^1COCH_2\text{-}CH_2\text{-}NR_2 + H_2O$), the Alder ene-reaction ($A\text{-}CH{=}CH_2 + R_2C{=}CH\text{-}C(R'_2)H \rightleftarrows A\text{-}CH_2\text{-}CH_2\text{-}C(R_2)\text{-}CH{=}C(R'_2)$), the alkylation of arenes by alkenes (e.g., $Ar\text{-}H + CH_2{=}CHR \rightleftarrows ArCH(Me)R$), the alkylation of alkenes with alkanes (e.g., the alkyl process, synthesis of isooctane from isobutene and isobutane), the hydroxyalkylation of alkenes by aldehydes (e.g., the Prins reaction $RCH{=}CH_2 + CH_2{=}O \rightleftarrows RCH{=}CH\text{-}CH_2OH$) [111,112], and the hydroxyalkylation of aromatic compounds with aldehydes. Other processes are catalyzed by a nucleophile (KCN, amine, phosphine, diaminocarbene) such as the benzoin condensation (e.g., 2 RCHO → RCH(OH)-COR), the Stetter reaction (e.g., $R^1CHO + R^2\text{-}CH{=}CH\text{-}COR^3 \rightarrow R^1CO(R^2)CH\text{-}CH_2\text{-}COR^3$), the Rahut-Currier reaction (e.g., $ArCOCH{=}CHCOOR + CH_2{=}CHCOMe \rightarrow ArCOCH_2CH(COOR)C(=CH_2)COMe$), and the Morita-Baylis-Hillman reaction (e.g., $R^1CHO + R^2CH{=}CHA \rightarrow R^1CH(OH)\text{-}C(A){=}CHR^2$ [113]. Since the discovery of the Fischer–Tropsch reactions (e.g., $nCO + (2n+1)H_2 \rightarrow nH_2O + C_nH_{(2n+2)}$) and the Roelen hydroformylation of alkenes ($RCH{=}CH_2 + CO + H_2 \rightarrow RCH_2CH_2CHO + RCH(CHO)Me$), transition metal-catalyzed hydrogenative C-C coupling reactions are taking more and more importance in fine organic synthesis [114–116]. Because it can be applied to a large variety of reactants and be asymmetric, Krische's hydrogenative coupling of dienes (or alkynes) with carbonyl compounds and imines (e.g., $CH_2{=}CH(R^1)CH{=}CH_2 + H_2 + R^2CHO \rightarrow CH_2{=}CH\text{-}C(Me)(R^1)\text{-}CH(OH)\text{-}R^2$) is a very powerful synthetic tool [117–121]. Alternatively, transition metal complexes can dehydrogenate primary alcohols and thus provide the corresponding aldehydes as an intermediates and, formally, H_2 necessary for the hydrogenative coupling of alkenes and aldehydes. Thus, one can use alcohols in the direct hydro(hydroxycarbation) of alkenes, 1,3-dienes, allenes and alkynes. The concept developed by Krische and co-workers is therefore a formal hydrocarbation (16) of unsaturated compounds by primary alcohols, a reaction that can simultaneously generate up to two new contiguous stereogenic centers [122–124].

$$H_2C{=}CR^1(R^2) + R^3CH_2\text{-}OH \rightarrow CH_3\text{-}C(R^1)(R^2)\text{-}CH(R^3)\text{-}OH \quad (16)$$

Krische defines the process as being a hydro(hydroxycarbation) via transfer hydrogenation. An example is given with Reaction (17) (Scheme 3). The alcohol equilibrates with its aldehyde and an iridium hydride that adds chemoselectively to the alkene generating a methyl(propargyl)iridium intermediates, which, in turn, adds to the intermediate aldehyde. When the transition metal catalyst is coordinated to an enantiomerically pure ligand, the hydro(hydroxycarbation) can be highly stereo-(dr = diastereoisomeric ratio) and enantioselective (ee = enantiomeric excess) [125,126].

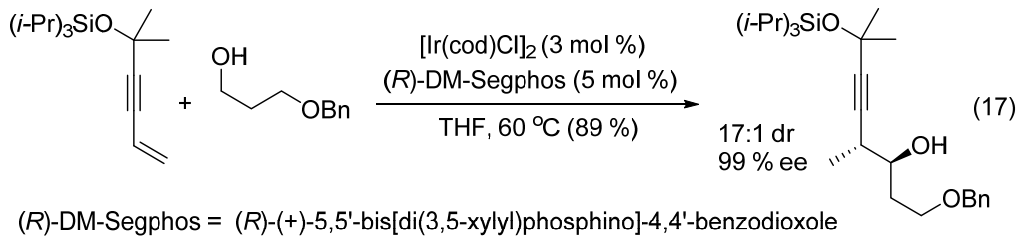

Scheme 3. Example of a regio-, stereo-, and enantioselective hydro(hydroxycarbation) of an alkene.

There have been many more exploratory studies on transition metal-catalyzed reactions than mechanistic studies. Thermochemical and kinetic data for transition metal complexes and their reactions are not as numerous as for organic compounds, but are being recorded more and more frequently. Nevertheless, because the structures and the reactions of transition metal complexes can be modeled by the structures and reactions of organic compounds, simple models are available to "classify" the reactions catalyzed by transition metal species.

In classical chemistry, direct hydrocarbations of unsaturated compounds X=Y are non-concerted processes. If R is an allyl moiety, a concerted ene-reaction can occur (e.g., CH_2=CH-CH_2R′ + X=Y → H-X-Y-CH_2-CH=CHR′). If the catalyst is a base B**:**, it deprotonates R-H forming the conjugate base R^- as an intermediate, which then adds to the alkene (or alkyne), generating an anionic adduct. The latter is then quenched by the conjugate acid BH^+ of the basic catalyst (nucleophilic addition (18)) or by R–H, realizing a chain process. Concurrently, the anionic adduct intermediate can add to another alkene (alkyne) and start the polymerization of the latter (anionic polymerization).

A second mechanism involves a radical intermediate $R^\bullet$ in which the catalyst is a radical or a species that can abstract a hydrogen atom from R-H. The addition of radical $R^\bullet$ to the alkene (alkyne) produces another radical that abstracts a hydrogen atom from H-X (radical addition (19)) or from R-H (chain process). Concurrently, the intermediate radical resulting from the initial radical addition can, in its turn, add to another alkene (alkyne) and lead to the polymerization of the latter (radical polymerization).

A third mechanism involves a cationic intermediate R^+ resulting from a hydride abstraction by a catalyst capable of abstracting a hydride from R-H reversibly. Such a mechanism corresponds to an electrophilic addition (20). Alternatively, the alkene can be protonated given a carbenium ion intermediate that adds to another alkene generating carbocationic adduct. At this stage, the latter is reduced by a hydride transfer from the alkane (e.g., the alkylate technology for the production of high octane number gasoline from a mixture of butene and isobutane) [127–131]. Concurrently, the first cationic adduct can add to another alkene, leading to its polymerization (cationic polymerization). Formally, instead of initiating the reaction by forming a carbenium ion intermediate R^+, one can imagine a catalyst M^+ that combines with R-H forming an organometallic species R-M and a proton. The protonation of the alkene (alkyne) follows, forming a carbenium ion that is quenched by R-M (Reaction (21), Figure 8), or that adds to another alkene (alkyne), starting its polymerization [132–139]. Mechanisms that involve a single electron transfer are also possible [140–142].

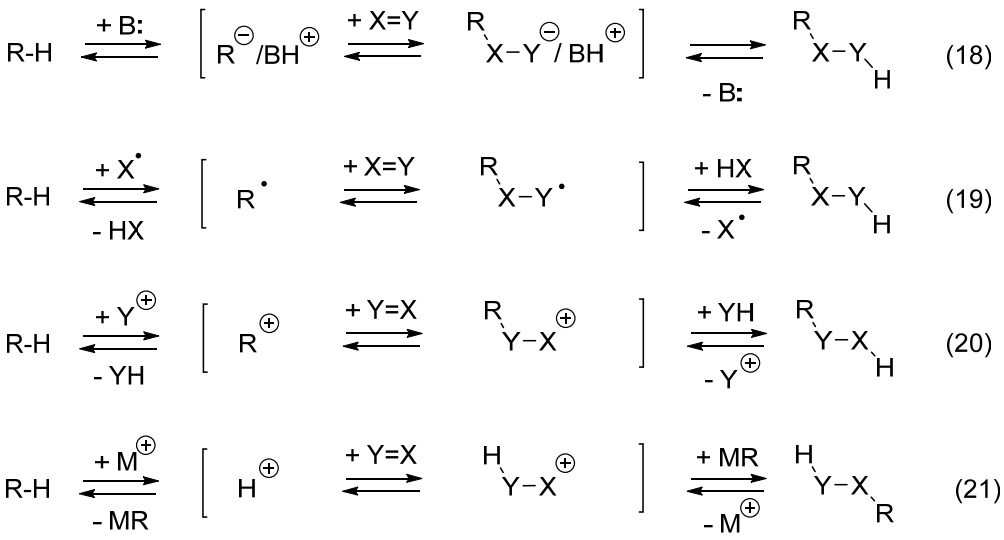

Figure 8. Classical general mechanisms for catalyzed hydrocarbations of unsaturated compounds. Polymerization of the unsaturated compound is a concurrent reaction.

11. Transition Metal-Catalyzed Hydrocarbations

Transition metal-catalyzed processes follow mechanisms in which several intermediates equilibrate with reactants and products. Thus, thermodynamics control the outcome of the process in many instances. Other transition-metal-catalytic reactions that are not reversible have rate-determining steps that determine the chemo-, regio-, stereo-, and enantioselectivity. The latter can be guessed, or quantum chemical calculations can help, at least in rationalizing the observations. A number of rules are available from thermochemical data; for instance, the M-C bonds are weaker than the M-H bonds, and the C-C bonds are weaker than the C-H bonds for comparable systems (same type of substitution). Scheme 4 with reaction (22) is generally retained for transition metal-catalyzed direct hydrocarbation of unsaturated compounds.

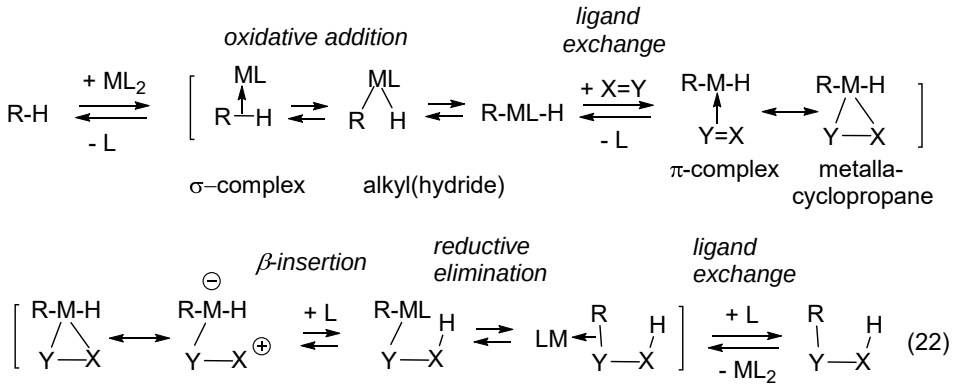

Scheme 4. Transition metal-catalyzed hydrocarbation of unsaturated systems.

Unsaturated transition metal complexes (with 16 or fewer valence electrons) are able to add across the σ(C-H) of R-H and form adducts of type R-[M]-H (can be an equilibrium of geometrical isomers) in which a σ(M-R) and a σ(M-H) bond are formed. In this adduct, the metal atom has gained two more valence electrons (VE) [143–147]. This is called an oxidative addition [148]. The oxidative addition (23) of a transition metal complex ML to a C-H bond is modeled in organic chemistry with the insertion of a carbene into a single C-H bond to give an alkane. For instance, methane adds to methylene carbene (reaction (24)), giving ethane ($\Delta_f H^\circ$ = standard heat of formation in the gas phase). The carbene has a carbon atom with a sextet of VE, meaning that it is unsaturated, whereas the carbon center in the product (alkane) has an octet of VE, meaning it is saturated. Another comparison is the reaction of a methyl cation with methane that equilibrates with an ethonium ion ($C_2H_7^+$ = protonated ethane) in the gas phase [149]. Dihydrogen (H_2) reacts with methyl cations (which has a sextet of VE on its carbon atom), giving a methonium ion (CH_5^+ = protonated methane, carbon atom with an octet of VE) as shown (Scheme 5) with Equilibrium (25) [150–154].

Transition metal complexes are good catalysts because they can exchange their ligand at relatively low temperature and assemble two reactants that must combine around the metal atom (template effect). Because bonds around the metallic center have bond angles that can be changed with little deformation energy, reactions that combine two reactants have relatively low energy barriers. Furthermore, the metallic center is highly polarizable, which means that it can take or give electrons very readily and at each step of the process.

The first and last steps of a transition-metal-catalytic process are ligand exchanges, as illustrated with the hydrocarbation reaction (22). The exchange of a ligand L (carbon monoxide, amine, phosphine, arsine, ether, aldehyde, ketone, alkene, alkyne, arenes, H_2, etc.) with an alkene (Reaction (26)) is modeled by the cyclopropanation of alkenes with methylene generated by photolysis of ketene (Reaction (27)), for instance, (Scheme 6). Another reaction to consider as a model is the formation of a *H*-cycloproponium ion by the addition of a methyl cation to an alkene (reaction (28)). *H*-cycloproponium ions

are intermediates (species longer-lived than transition structures) in Wagner–Meerwein rearrangements (see Table 1) [155].

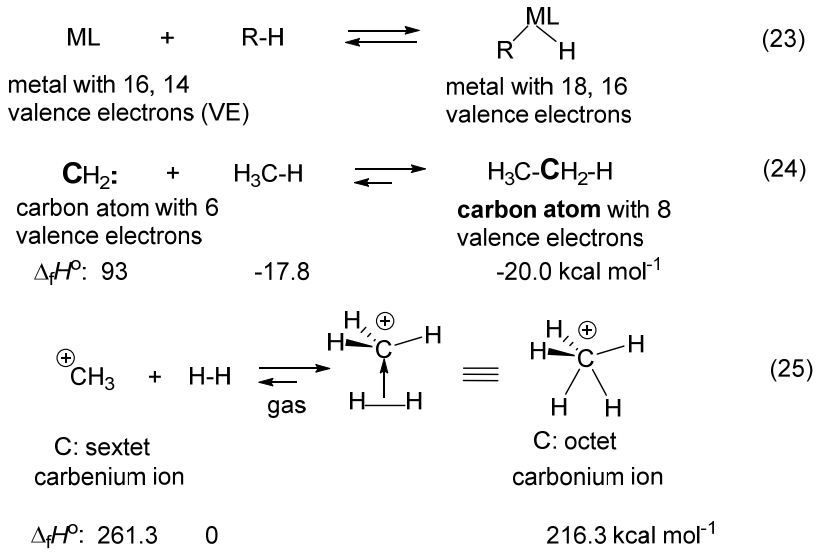

Scheme 5. 14, 16 VE transition metal complexes undergo oxidative additions to σ(X-H) bonds, as do carbene or carbenium ions (unsaturated 6 VE species).

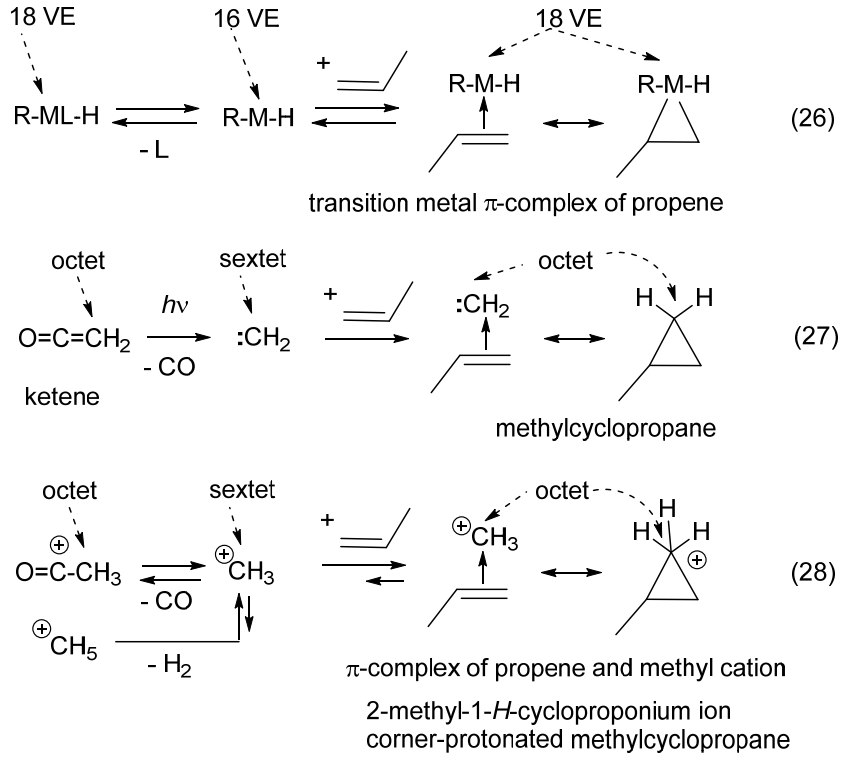

Scheme 6. 14, 16 VE transition complexes form π-complexes with unsaturated systems that can be seen as metallacyclopropanes, just as carbenes and carbenium ions (6 VE species) do with alkenes, generating cyclopropanes and protonated cyclopropanes, respectively.

Table 1. Fundamental reactions of transition metal complexes and comparison with organic reactions. Tolman's rules are applied to define (conventionally) the oxidation number x of the metal, M (VE: number of valence electrons). [M] = $M^{(x)}$ for a metal bearing other ligands eventually, including solvent molecules. Reprinted with permission from Ref. [17]. Copyright 2019 Wiley.

1. Ligand exchange

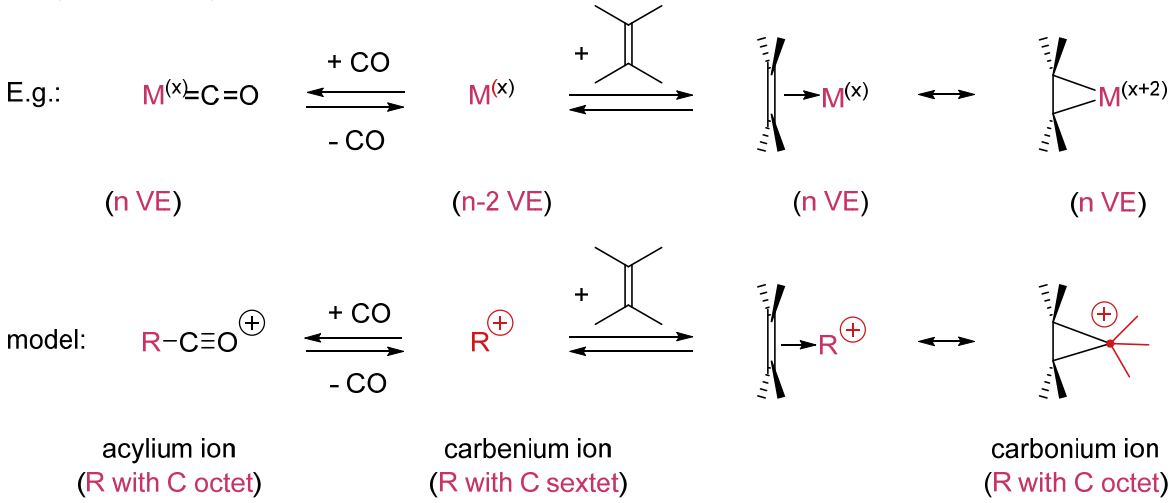

No change of valence electron count and oxidation number between the metal center of reactant [M]=CO and product [M](π-alkene) by convention.

2. Oxidative addition/reductive elimination

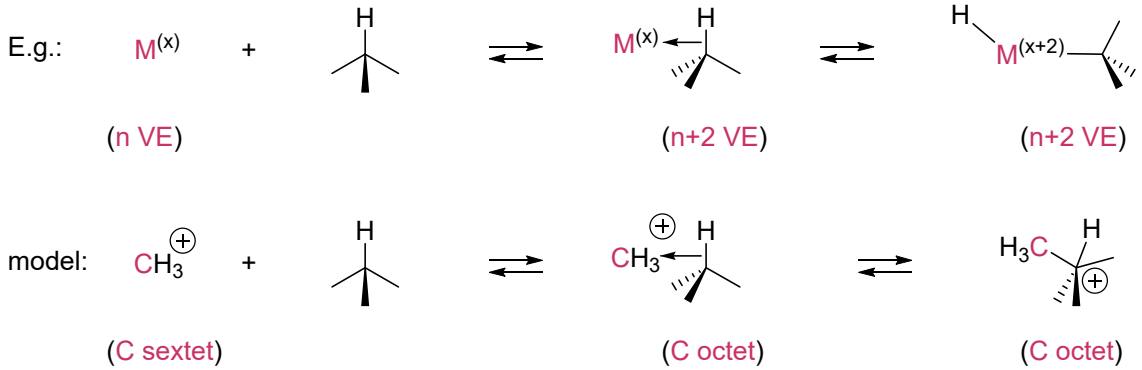

Oxidative addition requires an unsaturated metallic species (with 16, 14 VE). The metal oxidation number is increased by two and the metal of the adduct has two more VE than the metal in the starting complex. Note that unsaturated [M] can add to any kinds of X-Y bonds reversibly. The addition of carbenes R_2C: (C with a sextet) to X-H bonds generates stable compounds $R_2C(X)$-H with an octet carbon center. The opposite reaction is an α-elimination or 1,1-elimination.

3. α-Insertion/α-elimination

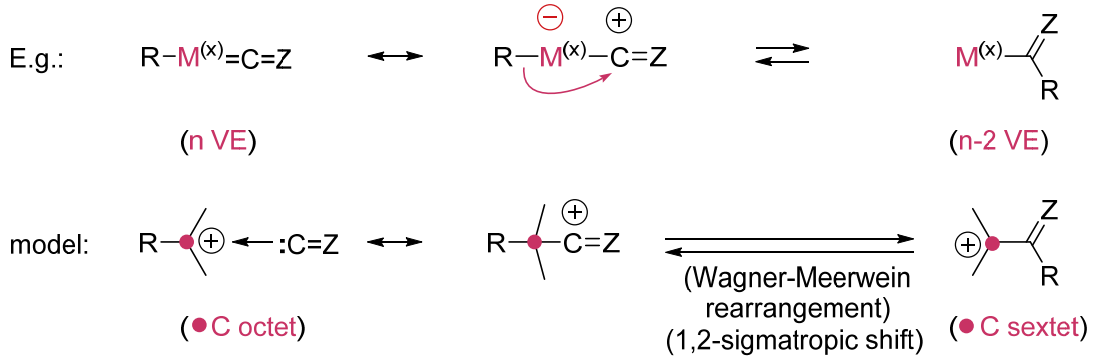

The number of VE is reduced by two when going from the reactant to the product in an α-insertion; the oxidation number of the metal is not changed (Z=O, NR', C(X)Y; R=H, alkyl, alkenyl, aryl, R'O, Hal, etc.).

Table 1. *Cont.*

4. β-Insertion/β-elimination

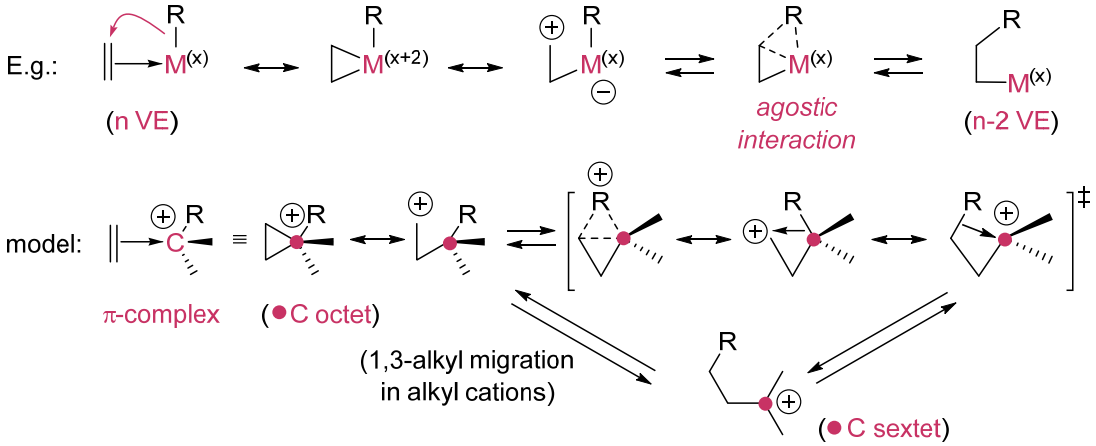

The number of VE is reduced by two when going from reactant to product in the β-insertion; the oxidation number of the metal is not changed (R = H, alkyl, alkenyl, aryl, R'O, Hal, etc.).

5. α-cycloinsertion/α-cycloelimination

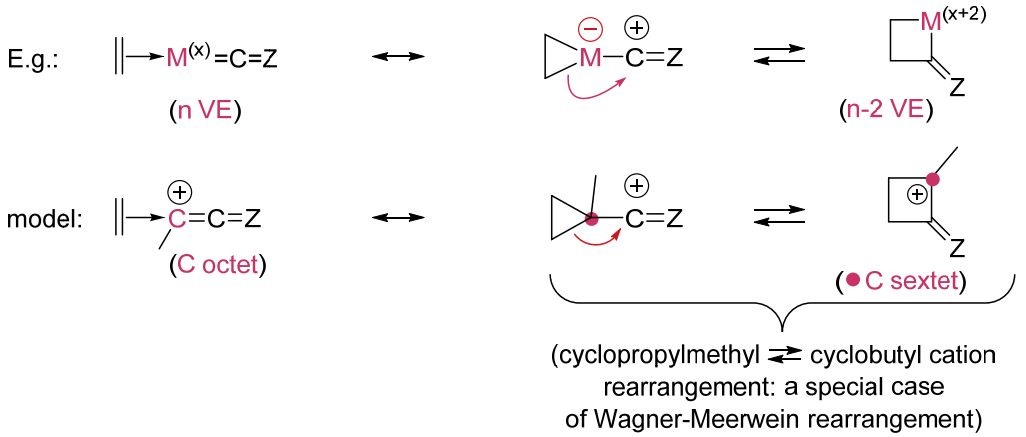

The number of VE of the metal is reduced by two when going from reactant to product in the α-cycloinsertion; the oxidation number of the metal is increased by two by convention.

6. Oxidative cyclization/reductive fragmentation (β-cycloinsertion/β-cycloelimination)

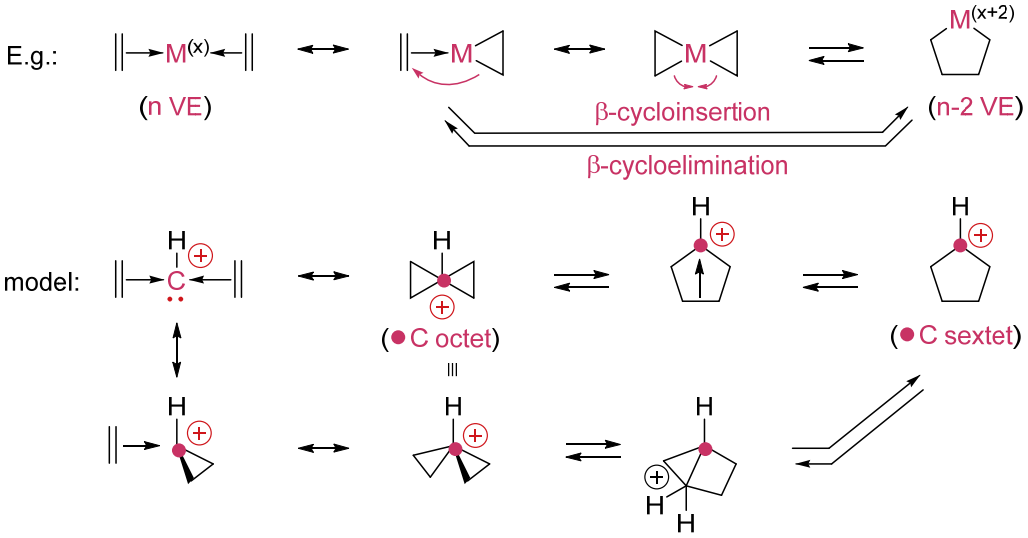

The number of VE of the metal is reduced by two when going from reactant to product in the oxidative cyclization and the oxidation number of the metal increases by two by convention. The metal-catalyzed cycloinsertions can combine other unsaturated reactants besides alkenes.

Table 1. *Cont.*

7. Reactions at the coordinated ligands

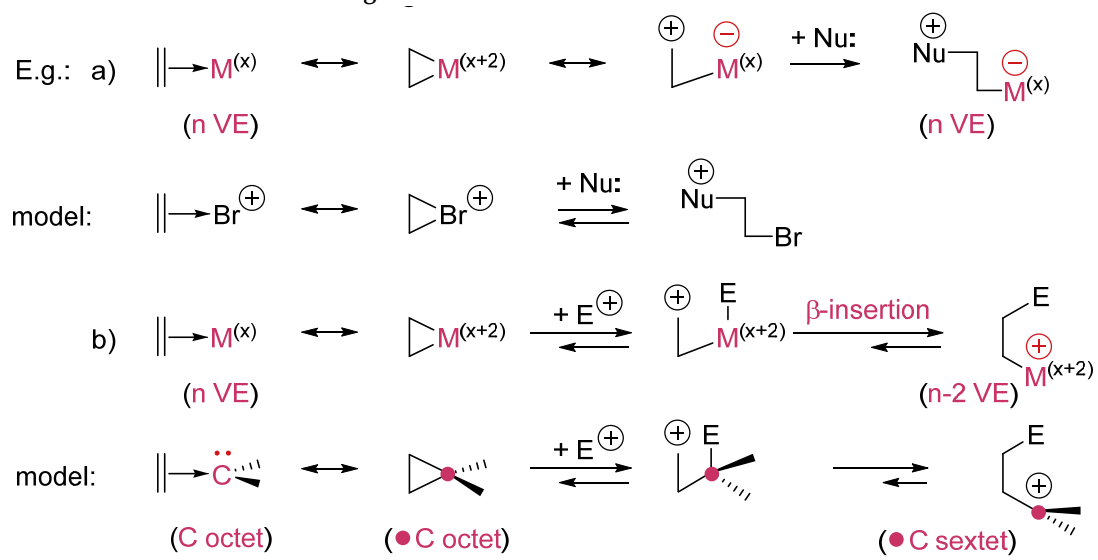

One of the processes that generates a bond between two reactants is the β-insertion (Reaction (30), the opposite reaction being a β-elimination). For the insertion of a hydrogen atom, the model reaction is the corner-to-corner migration in *H*-cycloproponium ions that corresponds to a 1,3-hydrogen shift, as shown with reaction (29) [156]. The rearrangement involves a transition structure that is a *C*-cycloproponium ion or edge-protonated cyclopropane (Scheme 7). A priori, any R group can do such migration (β-insertion). After the β-insertion, the metallic center has lost two VE. For the reaction to occur, a ligand L must coordinate the unsaturated metallic center.

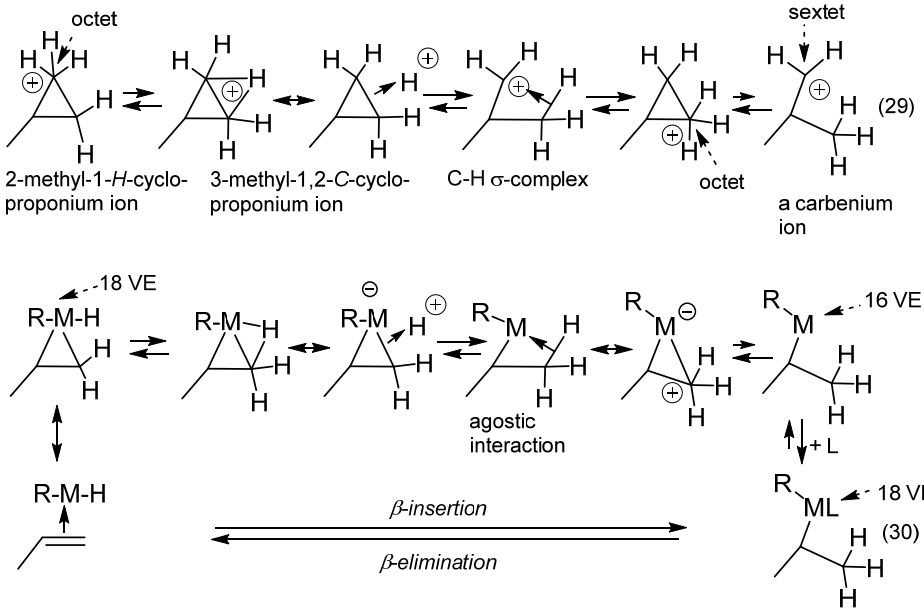

Scheme 7. β-insertions and β-eliminations in transition metal complexes are modeled by corner-to-corner migration in protonated cyclopropanes.

After the β-insertion, a reductive elimination (Reaction (31)), occurs, forming the final product of hydrocarbation and an unsaturated metallic species that can return as the active catalyst for another oxidative addition with reactant R-H, or be stabilized by

the coordination of a ligand molecule L of a solvent molecule (Scheme 8). The reductive elimination is the opposite reaction of the oxidative addition (e.g., Reaction (23)). If the 16-VE metallic adduct intermediate is an allylmetal species, it may add to the unsaturated system in a metalla-ene reaction [157,158].

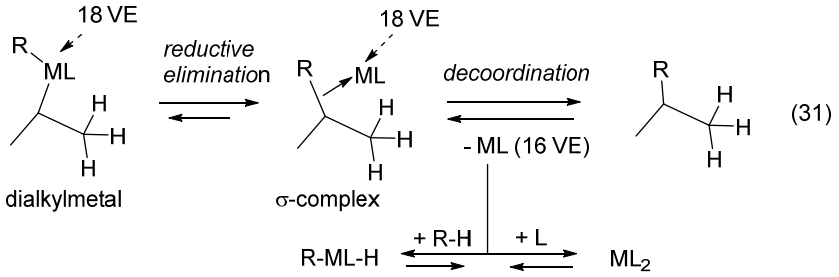

Scheme 8. β-Eliminations of transition metal complexes generate unsaturated species that are stabilized by coordination to an adequate ligand or solvent molecule.

The other processes (α-insertion/α-elimination, α-cycloinsertion/α-cycloelimination, β-cycloinsertion/β-cycloelimination) induced by transition metal complexes are also modeled by reactions of carbocations, as summarized in Table 1 [156].

12. Review of the Fundamental Reactions of Simple Carbocations

The mass spectrum of methane (CH_4) has peaks with mass/charge ratios m/Q = 12, 13, 14, 15, and 16 corresponding to the cations $C^{\bullet+}$, HC^+, $H_2C^{\bullet+}$, H_3C^+, and $H_4C^{\bullet+}$, respectively. The parent cation $H_4C^{\bullet+}$ (or molecular ion) can dissociate into hydrogen radical $H^\bullet$ and methyl cation H_3C^+, and so on. If there is sufficient pressure in the ionization chamber, the transfer of a proton (32) can take place (bimolecular reaction):

$$H_4C^{\bullet+} + CH_4 \rightarrow H_3C^\bullet + CH_5^+ \quad (32)$$

In this case, a peak is observed in the mass spectrum of methane with a mass/charge ratio m/Q = 17, which corresponds to methonium ion, CH_5^+, whose carbon atom is surrounded by an octet of valence electrons. It is much more stable (by 45 kcal mol^{-1}, Equilibrium (25)) than methyl cation, H_3C^+, whose carbon atom is surrounded by a sextet of valence electrons. Methonium ion is the prototype of carbonium ions. Methyl cation is the prototype of carbenium ions. The notation $H_4C^{\bullet+}$ describes the methanium radical-cation, which has seven valence electrons [159,160].

The salts of methyl and ethyl cations cannot be observed as persistent species in solution. When CD_3CH_2F is allowed to react with an excess of SbF_5/SO_2 at −78°C, complete deuterium/hydrogen scrambling in the ethyl group of ethyl fluoride is observed by ^{1}H-NMR spectroscopy. However, when CH_3CH_2F is added to DSO_3F/SbF_5 or DF/SbF_5 in SO_2 at −78°C, no detectable incorporation of deuterium into the ethyl group occurs [161]. This demonstrates that scrambling takes place intramolecularly in the ethyl cation intermediate (Scheme 9). Quantum calculations predict similar stabilities for classical ethyl cations and the bridged πH-ethenium ions (Equilibrium (33)) [162,163], which has been confirmed by infrared spectroscopy of the ion in the gas phase [164,165]. The πH-ethenium ion is the smallest possible π-complex of an alkene.

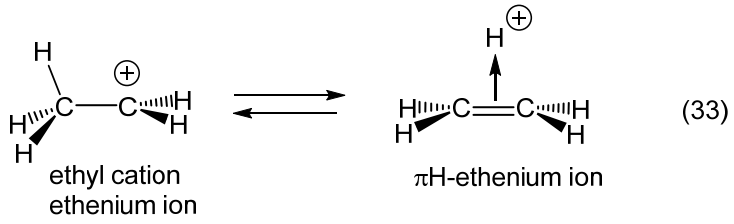

Scheme 9. Ethyl cations and πH-ethenium ions (π-complex of a proton with ethylene) have similar stabilities.

The simplest all-carbon and hydrogen carbenium ion prepared as a stable salt in solution is the *i*-propyl cation (Scheme 10). The 1,1,1-trideuterio-2-propyl cation (generated by treatment of 1,1,1-trideuterio-2-chloropropane in SbF_5/SO_2ClF at −110°C) rearranges (Equilibrium (34)) at −60°C into isomeric ions with Arrhenius activation parameters E_a = 16.4 ± 0.4 kcal mol^{-1} and log$A$ = 13.2 ± 0.3 [166]. The [2-^{13}C]prop-2-yl cation generated from [2-^{13}C]prop-2-yl chloride at low temperature was found to undergo intramolecular carbon scrambling between −90 and −60°C (Equilibrium (35)). This requires a process involving a corner-protonated cyclopropane or an edge-protonated cyclopropane intermediate (Equilibrium (36)) [167].

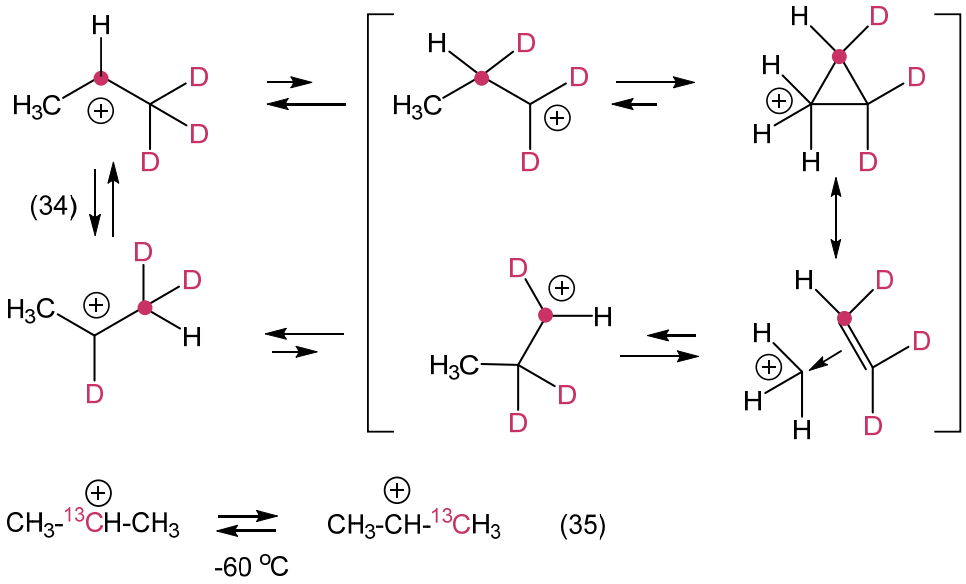

Scheme 10. Both the hydrogen- (Equilibrium (34)) and carbon-atom scrambling (Equilibrium (35)) are observed in isopropyl salt in a super-ionizing media (SbF_5/SO_2ClF).

The edge-protonated cyclopropane is somewhat higher in energy than the corner-protonated cyclopropane, although in the gas phase, fast scrambling (Equilibrium (36)) of hydrogen in protonated cyclopropane has been observed (Scheme 11) [168]. Infrared absorption features of gaseous isopropyl cations showed that corner-protonated cyclopropane is 8 kcal mol^{-1} less stable than isopropyl cations [169].

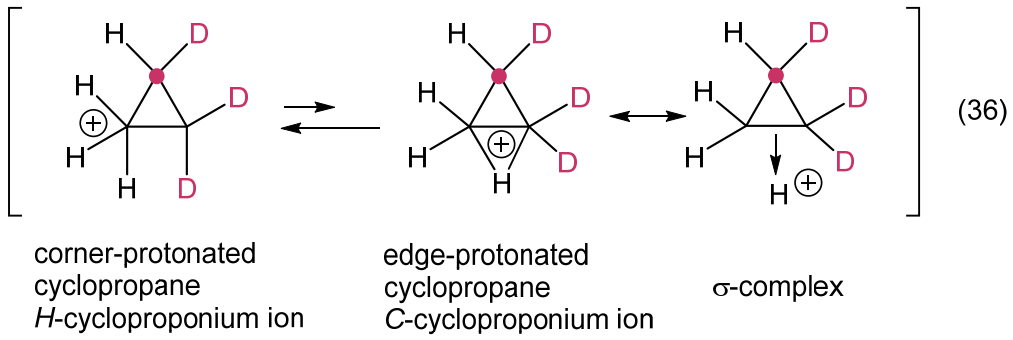

Scheme 11. Edge-protonated cyclopropane is slightly less stable than corner-protonated cyclopropane.

The ^{1}H-NMR spectrum of the but-2-yl cation (*s*-Bu$^+$) in SbF_5/SO_2ClF solution measured below −120°C indicates a very fast proton interchange due to Equilibrium (37) [170,171]. Between −100 and −40°C, all the hydrogen atoms in *s*-Bu$^+$ are scrambled with an activation energy E_a =7.5 ± 0.1 kcal mol^{-1} (log$A$ = 12.3 ± 0.1). If a series of 1,2-hydride shifts were responsible for the proton interchange, formation of a *n*-butyl (but-1-yl) cation intermediate (*n*-Bu$^+$) would be required (Scheme 12). However, by analogy with the isopropyl cation

(Equilibria (34) and (35)), the formation of *n*-Bu^+ would be expected to require an activation energy higher than 15 kcal mol^{-1}. Hence, a more facile process involving formation of a protonated methylcyclopropane and degenerate hydrogen shifts via an edge-protonated cyclopropane intermediate or transition state is more probable (Equilibrium (38)). When heated to −40 °C, the but-2-yl cation rearranges irreversibly into a *t*-butyl cation with an activation energy of 18 kcal mol^{-1}. The similarity of this energy barrier with that observed for the isopropyl ⇄ *n*-propyl cation rearrangement ($E_a \cong 16$ kcal mol^{-1}) indicates that the reaction takes place via the primary carbenium ion intermediate isobutyl cation, *i*-Bu^+, although this species is undoubtedly bridged by H or methyl in its minimum energy structure.

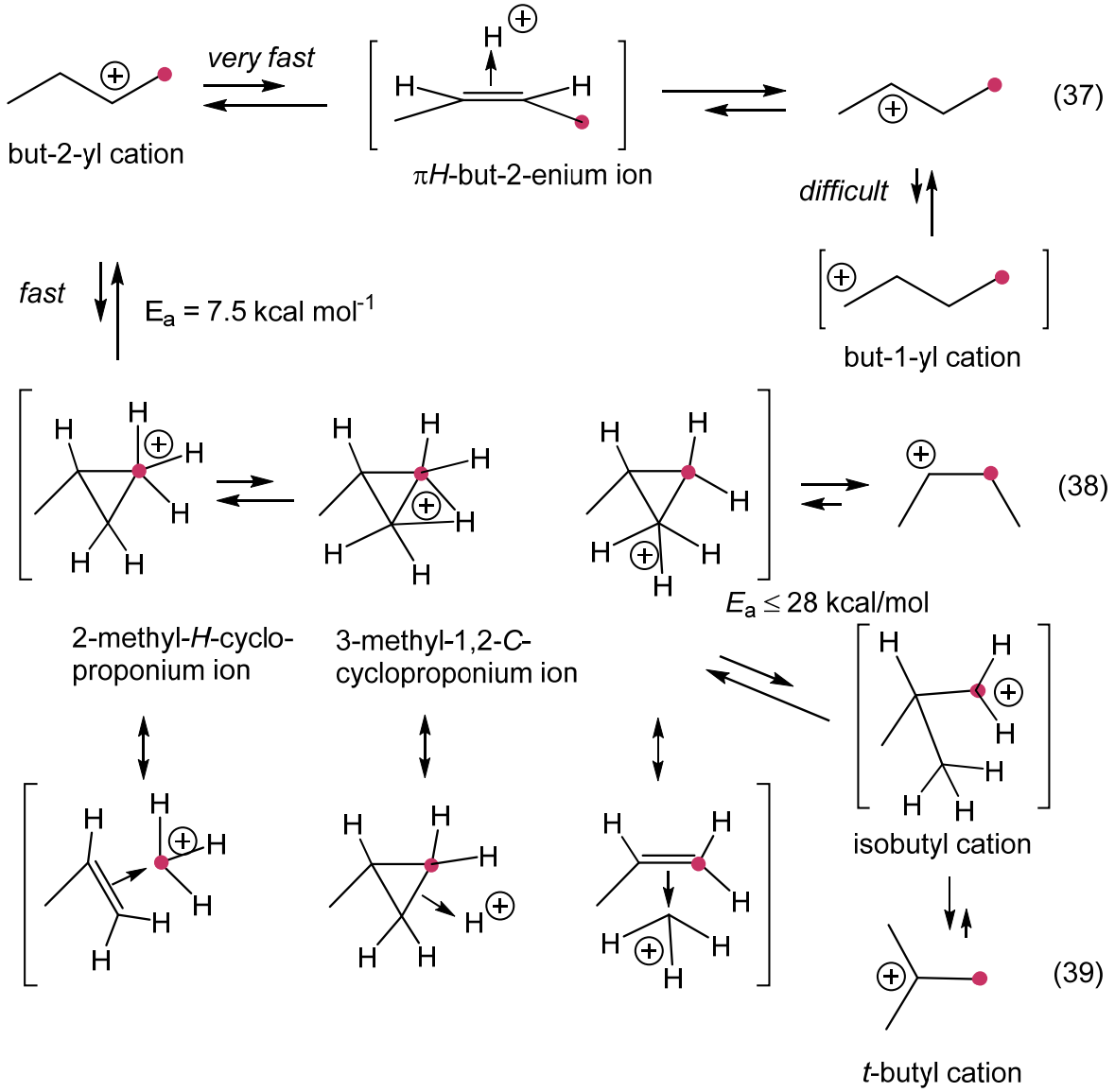

Scheme 12. Hydrogen- and carbon-atom scrambling in butyl salts in a super-ionizing medium (SbF_5/SO_2ClF).

Gas phase measurements indicate that the protonated cyclobutane is less stable than *s*-Bu^+, protonated methylcyclopropane and *n*-Bu^+ (Scheme 13) [172].

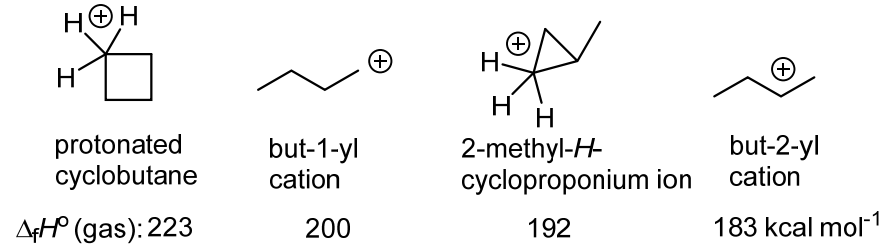

Scheme 13. Protonated cyclobutane is much less stable than protonated methylcyclopropane.

Two different types of hydrogen exchange processes have been observed in the ^{1}H-NMR spectrum of the *t*-amyl cation (2-methylbut-2-yl cation) (Scheme 14) [173]. One involves the interchange of the two types of methyl group protons, not affecting the methylene group (Equilibrium (40)). On the NMR time scale, this process occurs at temperatures above 0 °C and has an activation energy of $E_a \cong 15$ kcal mol^{-1} ($\log A \cong 13.2$). The rearrangement first involves a 1,2-sigmatropic shift of hydrogen generating a secondary alkyl cation intermediate (3-methylbut-2-yl cation). This is followed by a 1,2-sigmatropic shift of a methyl group (Wagner–Meerwein rearrangement) that generates another secondary alkyl cation intermediate (3-methylbut-2-yl cation). The latter undergoes a quick 1,2-sigmatropic shift of a hydrogen-producing *t*-amyl cation via a protonated dimethylcyclopropane (as intermediate or transition state). Since degenerate Wagner–Meerwein shifts of both hydrogen and methyl groups are very fast ($E_a < 4$ kcal/mol, see e.g., Equilibrium (37)) when no change in the degree of chain branching of the carbenium ion occurs, the major part of the activation energy for this rearrangement (15 kcal mol^{-1}) must be due to the formation of the secondary ion intermediate (3-methylbut-2-yl cation) from an *t*-amyl cation (2-methylbut-2-yl cation) [173].

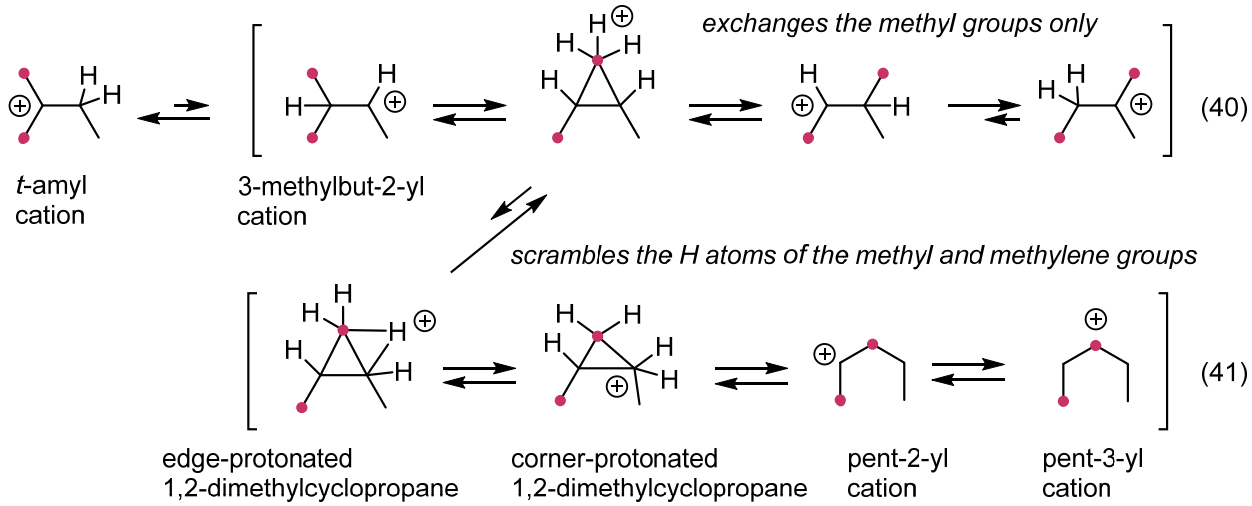

Scheme 14. Hydrogen- and carbon-atom scrambling in 2-methylbut-2-yl (tertioamyl) salt in a superionizing medium (SbF_5/SO_2ClF).

The second process (41) occurs above 80 °C on the NMR time scale. It causes the scrambling of all the hydrogen atoms in a *t*-amyl cation. It has an activation energy $E_a = 18.8 \pm 1$ kcal mol^{-1} ($\log A = 13.2 \pm 0.5$). A mechanism involving reversible hydride shifts to primary carbenium ion intermediates (e.g., 2-methylbut-1-yl cation) can be rejected on the basis that such species would have energies well above (*ca.* 30 kcal mol^{-1}) that of the starting tertiary cation (*t*-amyl cation). In the alternative mechanism shown with Equilibrium (41), the hydrogen atom interchange involves corner-to-corner hydrogen shifts in the protonated dimethylcyclopropane intermediates. Thus, this process, which involves an overall change in the degree of chain branching, has an energy barrier 3 kcal mol^{-1}

higher than those for related processes not involving such a change [155,174]. X-ray diffraction studies of crystals of a salt of 2-norbornyl cations ($[C_7H_{11}]^+$] $[Al_2Br_7]^-.CH_2Br_2$) at 40 K demonstrated this secondary alkyl cation adopting a C_s symmetrical structure, that is, a *H*-nortricyclonium cation (a corner-protonated cyclopropane) (Scheme 15) [175].

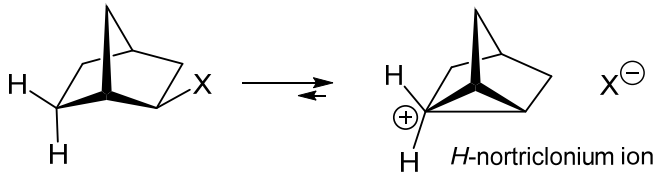

Scheme 15. The 2-norbornyl cation is a stable corner-protonated cyclopropane derivative (non-classical carbonium ion).

The secondary cyclopentyl cation is stable in SbF_5/SO_2ClF solution up to -20°C [176]. It undergoes a fast, degenerate 1,2-hydride shift (equilibrium (42), E_a < 4.5 kcal mol^{-1}), but no ring contraction (equilibrium (43)) has ever been detected (Scheme 16). Considering an energy difference of 15 kcal mol^{-1} for the isomerization of a secondary alkyl cation to a primary isomer and the ring strain difference of 20 kcal mol^{-1} between cyclopentane and cyclobutene, one estimates the cyclobutylmethyl cation to be less stable than the cyclopentyl cation by ca. 35 kcal mol^{-1}. Contrary to the cyclopropylmethyl cation, which is highly stabilized [177,178], the cyclobutylmethyl cation does not enjoy the same hyperconjugative stabilization [179,180].

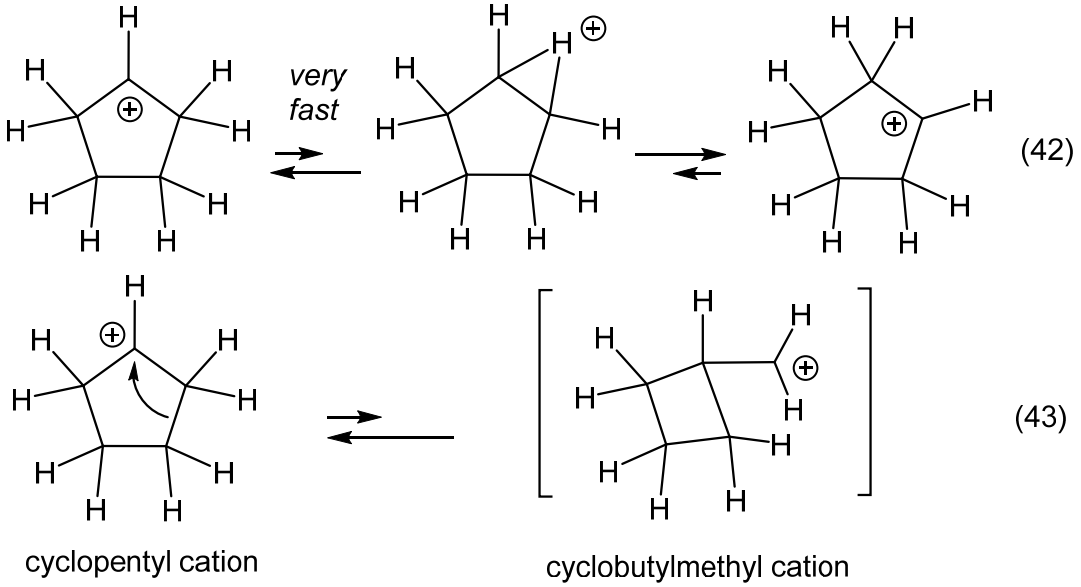

Scheme 16. The cyclobutylmethyl cation is not a stable primary carbenium ion.

In the gas phase, the doubly ^{13}C-labelled cyclopentyl cations **11** and **12** generated from the doubly ^{13}C-labelled bromides **7**–**10** undergo degenerate carbon scrambling (Equilibrium (44)) prior to elimination of ethylene (Fragmentation (45)). The complete carbon scrambling can, in principle, proceed via either the cyclobutylmethyl cation intermediate (Equilibrium (43)) or the "non-classical" pyramidal cation **13** (Equilibrium (44)), as calculations have suggested that they have similar energies [181,182]. Cation **13** can be viewed as a π-complex between ethylene and a cyclopropyl cation (corner-protonated spiropentane) or as a double π-complex between two ethylene units and the methylidynium ion, $:CH^+$ (Scheme 17). The fragmentation of the cyclopentyl cation into the allyl cation and ethylene (Fragmentation (45)) may also involve cation **13** as an intermediate. The dissociation of an ethylene unit from **13** via transition state **14** is expected to give an allyl cation and ethylene. This process would be analogous to the

gas phase fragmentation of the corner-protonated cyclopropane into molecular hydrogen and allyl cations. Mechanisms similar to those presented with Equilibrium (44) have been proposed to rationalize the complete hydrogen and carbon atom scrambling in the gaseous cyclohexyl ⇄ methylcyclopentyl cation equilibrium that occurs prior to monomolecular elimination of ethylene [183]. Cation **13** is also formed upon protonation of spiropentane. In the gas phase, its lifetime exceeds 7×10^{-9} s. Cation **13** is separated from the cyclopentyl cation by 30 kcal mol^{-1} [184,185].

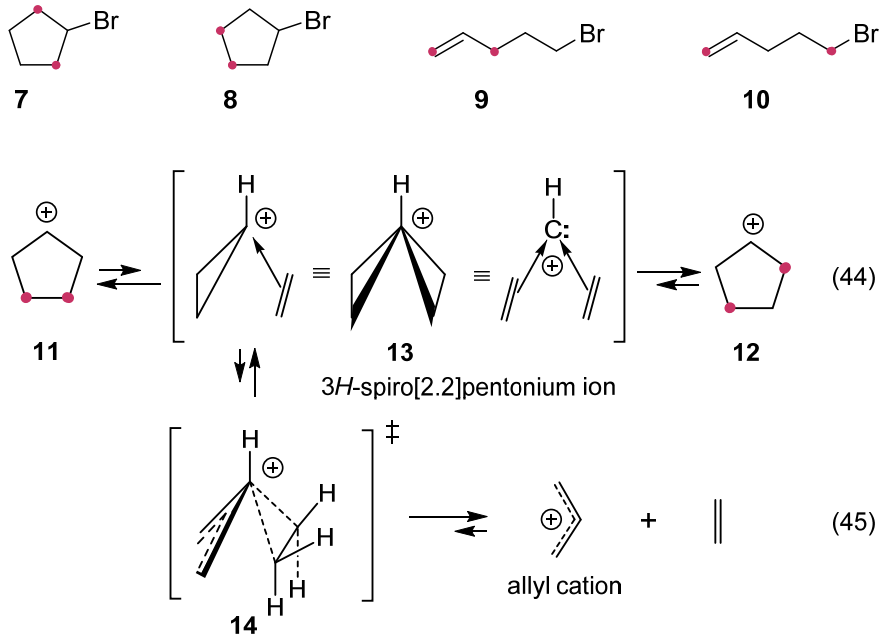

Scheme 17. In the gas phase, the cyclopentyl cation equilibrates with the corner-protonated spiropentane intermediate, which permits its carbon-atom scrambling and fragmentation into ethylene and an allyl cation.

13. Conclusions

The inventor of new processes can predict equilibrium constants and reaction rates by applying simple rules of thermodynamics and using published thermochemical data. Organic chemistry today offers a fantastic panoply of new reactions, especially catalytic reactions, that render the exploration of chemical space faster and more facile. Very important and sustainable processes are available, especially when atom economical processes are engaged, such as pericyclic reactions and direct hydrocarbation of unsaturated compounds. Catalysts can be invented that permit these reactions to be run under smooth conditions (no cooling, no heating, no solvent or in harmless solvents such as water, ethanol, ethyl acetate, or 2-methyltetrahydrofuran). There is a catalyst for any kind of reaction that permits energy savings and reduces the co-production of waste. The Vogel–Houk book has been written to help engineers and inventors realize a more sustainable world and to quickly generate a large number of new molecules that our civilization needs or will need. It also illustrates how fundamental concepts of chemical reactivity are based on thermodynamics. In this review, we have extracted a few models that help to show the analogies that exist between reactions of organic compounds and transition organometallic compounds. They help to understand a large number of catalyzed processes.

Author Contributions: Conceptualization, P.V. and K.N.H.; writing—original draft preparation, P.V.; writing—review and editing, P.V. and K.N.H. All authors have read and agreed to the published version of the manuscript.

Funding: The writing of this review was supported by the Basic Science Faculty of the "Ecole Polytechnique Fédérale de Lausanne" (EPFL) and by the Department of Chemistry and Biochemistry, University of California (UCLA), Los Angeles.

Acknowledgments: The authors thanks all their past and present co-workers and colleagues for their critical and fruitful discussions.

Conflicts of Interest: The authors declare no conflict of interest.

References

1. Perkin, W.H. LXXIV. On mauveine and allied colouring matters. *J. Chem. Soc. Trans.* **1879**, *35*, 717–732. [CrossRef]
2. Travis, A.S. Perkin's Mauve: Ancestor of the Organic Chemical Industry. *Technol. Cult.* **1990**, *31*, 51–82. [CrossRef]
3. Hubner, K. History–150 Years of mauveine. *Chem. Unserer Zeit* **2006**, *40*, 274–275. [CrossRef]
4. Liebig, J. Ueber die Zersetzung des Alkohols durch Chlor. *Ann. Der Pharm.* **1832**, *1*, 31–32. [CrossRef]
5. Butler, T.C. The introduction of chloral hydrate into medical practice. *Bull. Hist. Med.* **1970**, *44*, 168–172.
6. Jones, A.W. Early drug discovery and the rise of pharmaceutical chemistry. *Drug Test. Anal.* **2011**, *3*, 337–344. [CrossRef]
7. Ng, R. *Drugs: From Discovery to Approval*, 3rd ed.; John Wiley & Sons, Inc.: Hoboken, NJ, USA, 2015; pp. 1–560, ISBN 1118907272/9781118907276.
8. Inglis, L. *Milk of Paradise: A History of Opium*; Pan MacMillan: London, UK, 2019; pp. 1–440, ISBN 9781760782276.
9. Lev, E. Traditional healing with animals (zootherapy): Medieval to present-day Levantine practice. *J. Ethnopharmacol.* **2003**, *85*, 107–118. [CrossRef]
10. Bade, R.; Chan, H.-F.; Reynisson, J. Characteristics of known drug space, natural products, their derivatives and synthetic drugs. *Eur. J. Med. Chem.* **2010**, *45*, 5646–5652. [CrossRef]
11. Li, J.J. History of drug discovery. In *Drug Discovery*; Li, J.J., Corey, E.J., Eds.; John Wiley & Sons Inc.: Hoboken, NJ, USA, 2013; pp. 1–42.
12. Vogel, P. *Sustainable Development: The Roles of Carbon and Bio-Carbon; an Introduction to Molecular Sciences*; World Scientific Publishing: Hackensack, NJ, USA; London, UK; Singapore, 2022; pp. 1–585, ISBN 978-9811240485/9811240485.
13. Clayden, J.; Greeves, N.; Warren, S. *Organic Chemistry*, 2nd ed.; Oxford University Press: Oxford, UK, 2012; pp. 1–1234, ISBN 978-0199270293/0199270295.
14. Smith, M.B. *March's Advanced Organic Chemistry: Reactions, Mechanisms, and Structure*, 7th ed.; John Wiley & Sons. Inc.: Hoboken, NJ, USA, 2013; pp. 1–2047, ISBN 0470462590/1118854683/9788126556588/9780470462591/9781118854686/9788126556588.
15. Bruice, P.Y. *Organic Chemistry*, 8th ed.; Pearson Education: Upper Saddle River, NJ, USA, 2016; pp. 1–1344, ISBN 978-0134042282/013404228X.
16. Hartwig, J.F. *Organotransition Metal Chemistry. From Bonding to Catalysis*; University Science Books: Melville, NY, USA, 2010; pp. 1–1160, ISBN 978-1891389535.
17. Vogel, P.; Houk, K.N. *Organic Chemistry: Theory, Reactiviy and Mechanisms in Modern Synthesis*; Wiley-VCH Verlag GmbH & Co., KGaA: Weinheim, Germany, 2019; pp. 1–1352, ISBN 9783527345328/3527345329.
18. Anslyn, E.V.; Dougherty, D.A. *Modern Physical Organic Chemistry*; University Science Books: Sausalito, CA, USA, 2006; pp. 1–1095, ISBN 1891389319/9781891389313.
19. Wang, Z.; Wille, U.; Juaristi, E. (Eds.) *Encyclopedia of Physical Organic Chemistry*; John Wiley & Sons, Inc.: New York, NY, USA, 2017; Volume 6, pp. 1–4464, ISBN 978-1-118-47045-9.
20. Reymond, J.-L. The chemical space project. *Acc. Chem Res.* **2015**, *48*, 727–730. [CrossRef]
21. Awale, M.; Sirockin, F.; Stiefl, N.; Reymond, J.-L. Medicinal chemistry database GDBMedChem. *Mol. Inform.* **2019**, *38*, 1900031. [CrossRef]
22. Boström, J.; Brown, D.G. Stuck in a rut with old chemistry. *Drug Discov. Today* **2016**, *21*, 701–703. [CrossRef] [PubMed]
23. Brown, D.G.; Boström, J. Analysis of past and present synthetic methodologies on medicinal chemistry: Where have all the new reactions gone? *J. Med. Chem.* **2016**, *59*, 4443–4458. [CrossRef] [PubMed]
24. Jiang, X.; Hao, X.; Jing, L.; Wu, G.; Kang, D.; Liu, X.; Zhan, P. Recent applications of click chemistry in drug discovery. *Expert Opin. Drug Discov.* **2019**, *14*, 779–889. [CrossRef] [PubMed]
25. Takayama, Y.; Kusamori, K.; Nishikawa, M. Click chemistry as a tool for cell engineering and drug delivery. *Molecules* **2019**, *24*, 172. [CrossRef] [PubMed]
26. Dreher, S.D. Catalysis in medicinal chemistry. *Reaction Chem. Eng.* **2019**, *4*, 1530–1535. [CrossRef]
27. Siddiqui, S.; Sharma, S.; Sharma, B.; Siddiqui, A.A. Role of serendipity in drug discovery. *J. Pharm. Res.* **2010**, *9*, 49–55. [CrossRef]
28. Pedreira, J.G.B.; Franco, L.S.; Barreiro, E.J. Chemical intuition in drug design and discovery. *Curr. Top. Med. Chem.* **2019**, *19*, 1679–1693. [CrossRef]
29. NIST Chemistry WebBook, NIST Standard Reference Database Number 69, Last Update to Data 2022. Available online: https://webbook.nist.gov/chemistry/ (accessed on 15 May 2022).
30. Hendrickson, J.B. Systematic synthesis design. 4. Numerical codification of construction reactions. *J. Am. Chem. Soc.* **1975**, *97*, 5784–5800. [CrossRef]
31. Newhouse, T.; Baran, P.S.; Hoffmann, R.W. The economies of synthesis. *Chem. Soc. Rev.* **2009**, *38*, 3010–3021. [CrossRef]
32. Gaich, T.; Baran, P.S. Aiming for the ideal synthesis. *J. Org. Chem.* **2010**, *75*, 4657–4673. [CrossRef]

33. Morawetz, H.; Otaki, P.S. Kinetics and equilibria of amide formation in aqueous media. *J. Am. Chem. Soc.* **1963**, *85*, 463–468. [CrossRef]
34. de Azambuja, F.; Parac-Vogt, T.N. Water-tolerant and atom economical amide bond formation by metal-substituted polyoxometalate catalysts. *ACS Catal.* **2019**, *9*, 10245–10252. [CrossRef]
35. Perrot, P. *A to Z of Thermodynamics*; Oxford University Press: Oxford, UK; New York, NY, USA; Tokyo, Japan, 1998; pp. 1–336, ISBN 0198565569/9780198565567.
36. Kernen, P.; Vogel, P. The homoconjugated electron-releasing carbonyl group of 1-methyl-7-oxabicyclo[2.2.1]hept-5-en-2-one. Regioselective syntheses of 5-chloro- and 6-chloro-1-methyl-7-oxabicyclo[2.2.1]hept-5-en-2-one. *Helv. Chim. Acta* **1993**, *76*, 2338–2343. [CrossRef]
37. Vogel, P. The electron-releasing carbonyl group. Part 1: Discovery and theoretical studies. *Chim. Oggi* **1997**, *15*, 18–25.
38. Vogel, P. The electron-releasing carbonyl group. Part 2. Spectroscopic detection and synthetic applications. *Chim. Oggi* **1997**, *15*, 37–43. [CrossRef]
39. Carrupt, P.-A.; Vogel, P. Regioselective additions of electrophiles to olefins remotely perturbed–The carbonyl groups as a homoconjugated electron-donating substituent. *Tetrahedron Lett.* **1982**, *23*, 2563–2566. [CrossRef]
40. Carrupt, P.-A.; Vogel, P. The carbonyl group as homoconjugated electron-releasing substituent. Regioselective electrophilic additions at bicyclo[2.2.1]hept-5-en-2-one, bicyclo[2.2.2]oct-5-en-2-one, and derivatives. *Helv. Chim. Acta* **1989**, *72*, 1008–1028. [CrossRef]
41. Ruggiu, A.A.; Lysek, R.; Moreno-Clavijo, E.; Moreno-Vargas, A.J.; Robina, I.; Vogel, P. The regioselectivity of the addition of benzeneselenyl chloride to 7-azanorborn-5-ene-2-yl derivatives is controlled by the 2-substituent: New entry into 3- and 4-hydroxy-5-substituted prolines. *Tetrahedron* **2010**, *66*, 7309–7315. [CrossRef]
42. Carrupt, P.-A.; Vogel, P. The carbonyl group as homoconjugated electron-donating substituent–Ab initio STO3G MO calculations. *Tetrahedron Lett.* **1984**, *25*, 2879–2882. [CrossRef]
43. Sordo, J.A.; Varela-Alvarez, A.; Giani, S.; Vogel, P. Quantum calculations on the acid catalyzed rearrangements of norborn-5-en-2-one, 7-oxanorborn-5-en-2-one and 7-azanorborn-5-en-2-one. *Appl. Catal. A General* **2008**, *336*, 72–78. [CrossRef]
44. Le Drian, C.; Vogel, P. Acid-catalyzed rearrangement of 5,6-exo-epoxy-7-oxabicyclo[2.2.1]hept-2-yl derivatives–Migratory apitudes of acyl vs. alkyl groups in Wagner-Meerwein transpositions. *Helv. Chim. Acta* **1987**, *70*, 1703–1720. [CrossRef]
45. Berner, D.; Dahn, H.; Vogel., P. Unambiguous proof for alcoxycarbonyl group migration in Wagner-Meerwein rearrangements. *Helv. Chim. Acta* **1980**, *63*, 2538–2553. [CrossRef]
46. Scuseria, G.E.; Miller, M.D.; Jensen, F.; Geertsen, J. The dipole moment of carbon monoxide. *J. Chem. Phys.* **1991**, *94*, 6660–6663. [CrossRef]
47. De Proft, F.; Martin, J.M.L.; Geerlings, P. On the performance of density functional methods for describing atomic populations, dipole moments and infrared intensities. *Chem. Phys. Lett.* **1996**, *250*, 393–401. [CrossRef]
48. Abboud, J.L.M.; Alkorta, I.; Davalos, J.Z.; Müller, P.; Quintanilla, E. Thermodynamic stabilities of carbocations. *Adv. Phys. Org. Chem.* **2002**, *37*, 57–135. [CrossRef]
49. Aue, D.H. Carbocations. *Wiley Interdiscip. Rev.-Comput. Mol. Sci.* **2011**, *1*, 487–508. [CrossRef]
50. Klump, D.A. Carbocations. In *Organic Reaction Mechanisms Series*; Knipe, A.C., Ed.; Wiley Online Library, John Wiley & Sons, Inc.: Hoboken, NJ, USA, 2020; Chapter 6; pp. 337–367. [CrossRef]
51. Wodrich, M.D.; Wannere, C.S.; Mo, Y.; Jarowski, P.D.; Houk, K.N.; Schleyer, P.V.R. The concept of protobranching and its many paradigm shifting implications for energy evaluations. *Chem. Eur. J.* **2007**, *13*, 7731–7744. [CrossRef]
52. Aizman, A.; Contreras, R.; Galvan, M.; Cedillo, A.; Santos, J.C.; Chamorro, E. The Markovnikov regioselectivity rule in the light of site activation models. *J. Phys. Chem. A* **2002**, *106*, 7844–7849. [CrossRef]
53. Hughes, P. Was Markovnikov's rule an inspired guess? *J. Chem. Educ.* **2006**, *83*, 1152–1154. [CrossRef]
54. Kerber, R.C. Markovnikov's rule. *J. Chem. Educ.* **2007**, *84*, 1109. [CrossRef]
55. Ilich, P.P. Markovnikov's rule-Replies. *J. Chem. Educ.* **2007**, *84*, 1109. [CrossRef]
56. Zavitsas, A.A.; Rogers, D.W.; Matsunaga, N. Heats of formation of organic compounds by simple calculation. *J. Org. Chem.* **2010**, *75*, 6502–6515. [CrossRef] [PubMed]
57. Dimroth, O. Beziehungen zwischen Affinität und Reaktiongeschwindichkeit. *Angew. Chem.* **1933**, *52*, 571–576. [CrossRef]
58. Evans, M.G.; Polanyi, M. Further considerations on the thermodynamics of chemical equilibria and reaction rates. *Trans. Faraday Soc.* **1936**, *32*, 1333–1359. [CrossRef]
59. Bell, R.P. The kinetics of proton transfer reactions. *Trans. Faraday Soc.* **1938**, *34*, 0229–0236. [CrossRef]
60. Levy, D.E. *Arrow-Pushing in Organic Chemistry*, 2nd ed.; John Wiley & Sons, Inc.: Hoboken, NJ, USA, 2017; pp. 1–400. [CrossRef]
61. Woodward, R.B.; Hoffmann, R. Conservation of orbital symmetry. *Angew. Chem. Int. Ed.* **1969**, *8*, 781–853. [CrossRef]
62. Longuet-Higgins, H.C.; Abrahamson, E.W. The electronic mechanism of electrocyclic reactions. *J. Am. Chem. Soc.* **1965**, *87*, 2045–2046. [CrossRef]
63. Bickelhaupt, F.M.; Houk, K.N. Analyzing reaction rates with the distortion/interaction-activation strain model. *Angew. Chem. Int. Ed.* **2017**, *56*, 10070–10088. [CrossRef]
64. Dewar, M.J.S. Aromaticity and pericyclic reactions. *Angew. Chem. Int. Ed.* **1971**, *10*, 761–776. [CrossRef]
65. Zimmerman, H.E. Möbius-Hückel concept in organic chemistry-Application to organic molecules and reactions. *Acc. Chem. Res.* **1971**, *4*, 272–280. [CrossRef]

66. Evans, M.G. The activation energies of reactions involving conjugated systems. *Trans. Faraday Soc.* **1939**, *35*, 0824–0834. [CrossRef]
67. Houk, K.N. Frontier molecular orbital theory and organic reactions. *Nature* **1977**, *266*, 662. [CrossRef]
68. Lias, S.G.; Bartmess, J.E.; Liebman, J.F.; Holmes, J.L.; Levin, R.D.; Mallard, W.G. Gas-Phase Ion and Neutral Thermochemistry. *J. Phys. Chem. Reference Data* **1988**, *17* (Suppl. 1), 861. [CrossRef]
69. Rienstra-Kiracofe, J.C.; Tschumper, G.S.; Schaefer, H.F.I.; Nandi, S.; Ellison, G.B. Atomic and molecular electron affinities: Photoelectron experiments and theoretical computations. *Chem. Rev.* **2002**, *102*, 231–282. [CrossRef]
70. Dewar, M.J.S.; Pyron, R.S. Nature of transition state in some Diels-Alder reactions. *J. Am. Chem. Soc.* **1970**, *92*, 3098–3103. [CrossRef]
71. Dewar, J.J.S.; Pierini, A.B. Mechanism of the Diels-Alder reaction. Studies of the addition of maleic anhydride to furan and methylfurans. *J. Am. Chem. Soc.* **1984**, *106*, 203–208. [CrossRef]
72. Pedersen, S.; Herek, J.L.; Zewail, A.H. The validity of the diradical hypothesis-Direct femtosecond studies of the transition-state structures. *Science* **1994**, *266*, 1359–1364. [CrossRef]
73. Woodward, R.B.; Katz, T.J. The mechanism of the Diels-Alder reaction. *Tetrahedron* **1959**, *5*, 70–89. [CrossRef]
74. Horn, B.A.; Herek, J.L.; Zewail, A.H. Retro-Diels-Alder femtosecond reaction dynamics. *J. Am. Chem. Soc.* **1996**, *118*, 8755–8756. [CrossRef]
75. Littmann, E.R. The mechanism of the diene synthesis. *J. Am. Chem. Soc.* **1936**, *58*, 1316–1317. [CrossRef]
76. Houk, K.N.; Gonzalez, J.; Li, Y. Pericyclic reaction transition-states-Passions and punctilios, 1935–1995. *Acc. Chem. Res.* **1995**, *28*, 81–90. [CrossRef]
77. Houk, K.N. The frontier molecular orbital theory of cycloaddition reactions. *Acc. Chem. Res.* **1975**, *8*, 361–369. [CrossRef]
78. Chen, P.-P.; Ma, P.; He, X.; Svatunek, D.; Liu, F.; Houk, K.N. Computational exploration of ambiphilic reactivity of azides and Sustmann's paradigmatic parabola. *J. Org. Chem.* **2021**, *86*, 5792–5804. [CrossRef] [PubMed]
79. Gajewski, J.J.; Conrad, N.D. Variable transition-state structure in the Cope rearrangement as deduced from secondary deuterium kinetic isotope effects. *J. Am. Chem. Soc.* **1978**, *100*, 6269–6270. [CrossRef]
80. Hosomi, A.; Sakurai, H. Syntheses of γ,δ-unsaturated alcohols from allylsilanes and carbonyl compounds in presence of Ti tetrachloride. *Tetrahedron Lett.* **1976**, *17*, 1295–1298. [CrossRef]
81. Hosomi, A. Characteristics in the reactions of allylsilanes and their applications to versatile synthetic equivalents. *Acc. Chem. Res.* **1988**, *21*, 200–206. [CrossRef]
82. Biamonte, M.A. Sakurai allylation. In *Name Reactions for Homologation, Part I*; Li, J.J., Ed.; John Wiley & Sons, Inc.: Hoboken, NJ, USA, 2009; pp. 539–575, ISBN 0470487011/9780470487013.
83. Hayashi, T.; Kabeta, K.; Hamachi, I.; Kumada, M. Erythro-selectivity in addition of γ-substituted allylsilanes to aldehydes in the presence of Ti tetrachloride. *Tetrahedron Lett.* **1983**, *24*, 2865–2868. [CrossRef]
84. Deleris, G.; Dunoguès, J.; Calas, R. Synthèse d'alcools γ,δ-éthyléniques ou propargyliques par voie organosilicique. *Tetrahedron Lett.* **1976**, *28*, 2449–2450. [CrossRef]
85. Hoffmann, R.W.; Zeiss, H.J. Stereoselective synthesis of alcohols. 8. Diastereoselective synthesis of β-methylhomoallyl alcohols via crotylboronates. *J. Org. Chem.* **1981**, *46*, 1309–1314. [CrossRef]
86. Collum, D.B.; McDonald, J.H.; Still, W.C. Synthesis of the polyether antibiotic Monensin. 2. Preparation of intermediates. *J. Am. Chem. Soc.* **1980**, *102*, 2118–2120. [CrossRef]
87. Sato, F.; Iida, K.; Iijima, S.; Moriya, H.; Sato, M. Threo-selective synthesis of β-methylhomoallyl alcohols via but-2-enyltitanium compounds. *J. Chem. Soc. Chem. Commun.* **1981**, 1140–1141. [CrossRef]
88. Yamamoto, Y.; Maruyama, K. Crotylzirconium derivatives as a new reagent for the *threo*-selective synthesis of β-methylhomoallyl alcohols. *Tetrahedron Lett.* **1981**, *22*, 2895–2898. [CrossRef]
89. Hiyama, T.; Kimura, K.; Nozaki, H. Chromium(II) mediated *threo*-selective synthesis of homoallyl alcohols. *Tetrahedron Lett.* **1981**, *22*, 1037–1040. [CrossRef]
90. Yamamoto, Y.; Yatagai, H.; Naruta, Y.; Maruyama, K. *Erythro*-selective addition of crotyltrialkyltins to aldehydes regardless of the geometry of the crotyl unit-Stereoselection independent of the stereochemistry of precursors. *J. Am. Chem. Soc.* **1980**, *102*, 7107–7109. [CrossRef]
91. Shaik, S.S.; Pross, A. SN2 Reactivity of CH3X derivatives-A valence bond approach. *J. Am. Chem. Soc.* **1982**, *104*, 2708–2719. [CrossRef]
92. Pross, A. Relationship between rates and equilibria and the mechanistic significance of the Brønsted parameter-A qualitative valence-bond approach. *J. Org. Chem.* **1984**, *49*, 1811–1818. [CrossRef]
93. Shaik, S.S.; Schlegel, H.B.; Wolfe, S. *Theoretical Aspects of Physical Organic Chemistry. The SN2 Mechanism*; John Wiley & Sons Inc.: New York, NY, USA, 1992; pp. 1–285, ISBN 0471840416.
94. Shaik, S.S.; Ioffe, A.; Reddy, A.C.; Pross, A. Is the avoided crossing state a good approximation for the transition state of a chemical reaction-An analysis of Menschutkin and ionic SN2 reactions. *J. Am. Chem. Soc.* **1994**, *116*, 262–273. [CrossRef]
95. Pross, A. *Theoretical & Physical Principles of Organic Reactivity*; John Wiley & Sons, Inc.: New York, NY, USA, 1995; pp. 1–312. ISBN 0471555991/9780471555995.
96. Anglada, J.M.; Besalú, E.; Bofill, J.M.; Crehuet, R. Prediction of approximate transition states by Bell-Evans-Polanyi principle: I. *J. Comput. Chem.* **1999**, *20*, 1112–1129. [CrossRef]

97. Bofill, J.M.; Anglada, J.M.; Besalú, E.; Crehuet, R. Quantum chemical reactivity: Beyond the study of small molecules. In *Fundamentals of Molecular Similarity*; Springer: Boston, MA, USA, 2001; pp. 125–141. [CrossRef]
98. Wester, R.B.A.E.; Davis, A.V.; Neumark, D.M. Time-resolved study of the symmetric SN2-reaction I-+CH3I. *J. Chem. Phys.* **2003**, *119*, 10032–10039. [CrossRef]
99. Smith, M.B. Aliphatic Substitution, Nucleophilic and Organometallic. In *March's Advanced Organic Chemistry, Reactions, Mechanisms, and Structure*; John Wiley & Sons, Inc.: Hoboken, NJ, USA, 2013; Chapter 10; pp. 373–568. [CrossRef]
100. Crampton, M.R. Electrophilic aromatic substitution. In *Organic Reaction Mechanisms Series*; Knipe, A.C., Ed.; John Wiley & Sons: Hoboken, NJ, USA, 2014; Chapter 6; pp. 257–283. [CrossRef]
101. Rowlands, G.J. Radicals in organic synthesis: Part 2. *Tetrahedron* **2010**, *66*, 1593–1636. [CrossRef]
102. Tebben, L.; Studer, A. Nitroxides: Applications in synthesis and in polymer chemistry. *Angew. Chem. Int. Ed.* **2011**, *50*, 5034–5068. [CrossRef] [PubMed]
103. Quiclet-Sire, B.; Zard, S.Z. Fun with radicals: Some new perspectives for organic synthesis. *Pure Appl. Chem.* **2011**, *83*, 519–551. [CrossRef]
104. Lapointe, G.; Kapat, A.; Weidner, K.; Renaud, P. Radical azidation reactions and their application in the synthesis of alkaloids. *Pure Appl. Chem.* **2012**, *84*, 1633–1641. [CrossRef]
105. Sebren, L.J.; Devery, J.J.; Stephenson, C.R. Catalytic radical domino reactions in organic synthesis. *ACS Catal.* **2014**, *4*, 703–716. [CrossRef]
106. Denes, F.; Pichowicz, M.; Povie, G.; Renaud, P. Thiyl radicals in organic synthesis. *Chem. Rev.* **2014**, *114*, 2587–2693. [CrossRef]
107. Smith, M.B. Addition to carbon-carbon multiple bonds. In *March's Advanced Organic Chemistry, Reactions, Mechanisms, and Structure*; John Wiley & Sons, Inc.: Hoboken, NJ, USA, 2013; Chapter 15; pp. 859–902. [CrossRef]
108. Trost, B.M. The atom economy—A search for synthetic efficiency. *Science* **1991**, *254*, 1471–1477. [CrossRef]
109. Shin, I.; Montgomery, T.P.; Krische, M.J. Catalytic C-C bond formation and the Hendricksonian ideal: Atom- and redox-economy, stereo- and site-selectivity. *Aldrichimica Acta* **2015**, *48*, 15.
110. Smith, M.B. *March's Advanced Organic Chemistry: Reactions, Mechanisms, and Structure*, 8th ed.; John Wiley & Sons. Inc.: Hoboken, NJ, USA, 2022; Chapters 15 & 16; pp. 891–1272, ISBN 978-1119371809/1119371805.
111. Arundale, E.; Mikeska, L.A. The olefin aldehyde condensation-The Prins reaction. *Chem. Rev.* **1952**, *51*, 505–555. [CrossRef]
112. Overman, L.E.; Velthuisen, E.J. Scope and facial selectivity of the Prins-pinacol synthesis of attached rings. *J. Org. Chem.* **2006**, *71*, 1581–1587. [CrossRef]
113. Li, C.J. The development of catalytic nucleophilic additions of terminal alkynes in water. *Acc. Chem. Res.* **2010**, *43*, 581–590. [CrossRef]
114. Engle, K.M.; Mei, T.S.; Wasa, M.; Yu, J.Q. Weak coordination as a powerful means for developing broadly useful C-H functionalization reactions. *Acc. Chem. Res.* **2012**, *45*, 788–802. [CrossRef] [PubMed]
115. Colby, D.A.; Tsai, A.S.; Bergman, R.G.; Ellman, J.A. Rhodium-catalyzed chelation-assisted C-H bond functionalization reactions. *Acc. Chem. Res.* **2012**, *45*, 814–825. [CrossRef] [PubMed]
116. Rogge, T.; Kaplaneris, N.; Chatani, N.; Kim, J.; Chang, S.; Punji, B.; Schafer, L.L.; Musaev, D.G.; Wencel-Delord, J.; Roberts, C.A.; et al. C-H activation. *Nat. Rev. Methods Primers* **2021**, *1*, 43. [CrossRef]
117. Jang, H.Y.; Huddleston, R.R.; Krische, M.J. Reductive generation of enolates from enones using elemental hydrogen: Catalytic C-C bond formation under hydrogenative conditions. *J. Am. Chem. Soc.* **2002**, *124*, 15156–15157. [CrossRef] [PubMed]
118. Jang, H.Y.; Krische, M.J. Catalytic hydrogen-mediated cross-coupling of enones and carbonyl compounds: Aldol condensation by hydrogenation. *Eur. J. Org. Chem.* **2004**, *2004*, 3953–3958. [CrossRef]
119. Ngai, M.Y.; Kong, J.R.; Krische, M.J. Hydrogen-mediated C-C bond formation: A broad new concept in catalytic C-C coupling. *J. Org. Chem.* **2007**, *72*, 1063–1072. [CrossRef]
120. Nguyen, K.D.; Park, B.Y.; Luong, T.; Sato, H.; Garza, V.J.; Krische, M.J. Metal-catalyzed reductive coupling of olefin-derived nucleophiles: Reinventing carbonyl addition. *Science* **2016**, *354*, 300. [CrossRef]
121. Holmes, M.; Schwartz, L.A.; Krische, M.L. Intermolecular metal-catalyzed reductive coupling of dienes, allenes, and enynes with carbonyl compounds and imines. *Chem. Rev.* **2018**, *118*, 6026–6052. [CrossRef]
122. Ngai, M.Y.; Rucas, E.; Krische, M.J. Ruthenium-catalyzed C-C bond formation via transfer hydrogenation: Branch-selective reductive coupling of allenes to paraformaldehyde and higher aldehydes. *Org. Lett.* **2008**, *10*, 2705–2708. [CrossRef]
123. Shibahara, F.; Bower, J.F.; Krische, M.J. Ruthenium-catalyzed C-C bond forming transfer hydrogenation: Carbonyl allylation from the alcohol or aldehyde oxidation level employing acyclic 1,3-dienes as surrogates to preformed allyl metal reagents. *J. Am. Chem. Soc.* **2008**, *130*, 6338–6339. [CrossRef]
124. Sam, B.; Breit, B.; Krische, M.J. Paraformaldehyde and methanol as C1 feedstocks in metal-catalyzed C-C couplings of -unsaturated reactants: Beyond hydroformylation. *Angew. Chem. Int. Ed.* **2015**, *54*, 3267–3274. [CrossRef] [PubMed]
125. Geary, L.M.; Woo, S.K.; Leung, J.C.; Krische, M.J. Diastereo- and enantioselective Ir-catalyzed carbonyl propargylation from the alcohol or aldehyde oxidation level: 1,3-Enynes as allenylmetal equivalents. *Angew. Chem. Int. Ed.* **2012**, *51*, 2972–2976. [CrossRef] [PubMed]
126. Nguyen, K.D.; Herkommer, D.; Krische, M.J. Ruthenium-BINAP catalyzed alcohol C-H *tert*-prenylation via 1,3-enyne transfer hydrogenation: Beyond stoichiometric carbanions in enantioselective carbonyl propargylation. *J. Am. Chem. Soc.* **2016**, *138*, 5238–5241. [CrossRef] [PubMed]

127. Speith, J.G. *The Chemistry and Technology of Petroleum*; CRC Press, Francis & Taylor Group: Boca Raton, FL, USA, 2006; pp. 1–984, ISBN 1420008382/9781420008388.
128. Corma, A.; Martínez, A. Chemistry, catalysts, and processes for isoparaffin–olefin alkylation: Actual situation and future trends. *Rev. Sci. Eng.* **1993**, *35*, 483–570. [CrossRef]
129. Li, X.; Nagoaka, K.; Simon, L.J.; Olindo, R.; Lercher, J.A. Mechanism of butane skeletal isomerization on sulfated zirconia. *J. Catal.* **2005**, *232*, 456–466. [CrossRef]
130. Wang, P.; Zhang, J.; Wang, G.; Li, C.; Ang, C. Nature of active sites and deactivation mechanism for *n*-butane isomerization over alumina-promoted sulfated zirconia. *J. Catal.* **2016**, *338*, 124–134. [CrossRef]
131. Olah, G.A.; Farooq, O.; Husain, A.; Ding, N.; Trivedi, N.J.; Olah, J.A. Superacid FSO3H/HF catalyzed butane isomerization. *Catal. Lett.* **1991**, *10*, 239–247. [CrossRef]
132. Kennedy, J.P. Living cationic polymerization of olefins. How did the discovery come about. *J. Polym. Sci. Part A Polym. Chem.* **1999**, *37*, 2285–2293. [CrossRef]
133. Puskas, J.E.; Peng, H.H. Kinetic simulation of living carbocationic polymerizations. I. Simulation of living isobutylene polymerization. *Polym. React. Eng.* **1999**, *7*, 553–576. [CrossRef]
134. Rudin, A.; Choi, P. *The Elements of Polymer Science and Engineering*, 3rd ed.; Academic Press: New York, NY, USA; Elsevier: Amsterdam, The Netherlands, 2013; pp. 1–563, ISBN 978-0-12-382178-2.
135. Vasilenko, I.V.; Yeong, H.Y.; Delgado, M.; Ouardad, S.; Peruch, F.; Voit, B.; Ganachaud, F.; Kostjuk, S.V. A catalyst platform for unique cationic (co)polymerization in aqueous emulsion. *Angew. Chem. Int. Ed.* **2015**, *54*, 12728–12732. [CrossRef]
136. Ouardad, S.; Wirotius, A.L.; Kostjuk, S.; Ganachaud, F.; Peruch, F. Carbocationic polymerization of isoprene using cumyl initiators: Progress in understanding side reactions. *RSC Adv.* **2015**, *5*, 59218–59225. [CrossRef]
137. Goriainow, W.; Butlerow, A. Ueber die Polyolene und die Umwandlung von Aethylen in Aethylalkohol. *Liebigs Ann. Chem.* **1873**, *169*, 146–149. [CrossRef]
138. Kostjuk, S.V. Recent progress in the Lewis acid co-initiated cationic polymerization of isobutylene with 1,3-dienes. *RSC Advances* **2015**, *5*, 13125–13144. [CrossRef]
139. Rajasekhar, T.; Singh, G.; Kapur, G.S.; Ramakumar, S.S.V. Recent advances in catalytic chain transfer polymerization of isobutylene: A review. *RSC Adv.* **2020**, *10*, 18180–18191. [CrossRef]
140. Mattay, J. Photo-induced electron-transfer in organic synthesis. *Synthesis* **1989**, *1989*, 233–256. [CrossRef]
141. Garcia, H.; Roth, H.D. Generation and reactions of organic radical-cations in zeolites. *Chem. Rev.* **2002**, *102*, 3977–4007. [CrossRef] [PubMed]
142. Broggi, J.; Rollet, M.; Clément, J.-L.; Canard, G.; Terme, T.; Gigmes, D.; Vanelle, P. Polymerization initiated by organic electron donors. *Angew. Chem. Int. Ed.* **2016**, *55*, 5994–5999. [CrossRef]
143. Elschenbroich, C. *Organometallics, 3rd Completely Revised and Extended Edition*; Wiley-VCH Verlag GmbH & Co. KGaA: Weinheim, Germany, 2006; pp. 1–817, ISBN 978-3-527-29390-2.
144. Ishii, Y.; Tsutsui, M. *Organotransition-Metal Chemistry*; Springer: Boston, MA, USA, 1975; pp. 1–398. [CrossRef]
145. Crabtree, R.H. An organometallic future in green and energy chemistry? *Organometallics* **2011**, *30*, 17–19. [CrossRef]
146. Mathey, F. *Transition Metal Organometallic Chemistry*; SpringerBriefs in Molecular Sciences; Springer: Singapore, 2013; pp. 1–100, ISBN 978-981-4451-09-3.
147. Frenking, G. Chemical bonding in transition metals. In *The Chemical Bond: Chemical Bonding Across the Periodic Table*; Frenking, G., Sason, S., Eds.; Wiley-VCH Verlag GmbH & Co. KGaA: Weinheim, Germany, 2014; pp. 175–218. [CrossRef]
148. Tolman, C.A. 16 and 18 electron rule in organometallic chemistry and homogeneous catalysis. *Chem. Soc. Rev.* **1972**, *1*, 337–353. [CrossRef]
149. Carneiro, J.W.d.M.; Schleyer, P.V.R.; Saunders, M.; Remington, R.; Schaefer, H.F., III; Rauk, A.; Sorensen, T.S. Protonated ethane. A theoretical investigation of C2H7+ structures and energies. *J. Am. Chem. Soc.* **1994**, *116*, 3483–3493. [CrossRef]
150. Smith, D.; Adams, N.G.; Alge, E. Isotope exchange and collisional association in the reactions of CH_3^+ and its deuterated analogs with H2, HD, and D2. *J. Chem. Phys.* **1982**, *77*, 1261–1268. [CrossRef]
151. White, E.T.; Tang, J.; Oka, T. CH_5^+: The infrared spectrum observed. *Science* **1999**, *284*, 135–137. [CrossRef] [PubMed]
152. Huang, X.C.; Johnson, L.M.; Bowman, J.M.; McCoy, A.B. Deuteration effects on the structure and infrared spectrum of CH_5^+. *J. Am. Chem. Soc.* **2006**, *128*, 3478–3479. [CrossRef]
153. Hinkle, C.E.; McCoy, A.B. Isotopic effects on the dynamics of the $CH_3^+ + H_2 \rightarrow CH_5^+ \rightarrow CH_3^+ + H_2$ reaction. *J. Phys. Chem. A* **2012**, *116*, 4687–4694. [CrossRef] [PubMed]
154. Asvany, O.; Yamada, K.M.T.; Bruenken, S.; Potapov, A.; Schlemmer, S. Experimental ground-state combination differences of CH_5^+. *Science* **2015**, *347*, 1346–1349. [CrossRef] [PubMed]
155. Saunders, M.; Vogel, P.; Hagen, E.L.; Rosenfeld, J. Evidence for protonated cyclopropane intermediates from studies of stable solutions of carbonium ions. *Acc. Chem. Res.* **1973**, *6*, 53–59. [CrossRef]
156. Vogel, P. Carbocation Chemistry. In *Studies in Organic Chemistry*; Elsevier: Amsterdam, The Netherlands, 1985; pp. 1–596, ISBN 0444425225.
157. Cabrera, J.M.; Krische, M.J. Total synthesis of clavosolide A via asymmetric alcohol-mediated carbonyl allylation: Beyond protecting groups or chiral auxiliaries in polyketide construction. *Angew. Chem. Int. Ed.* **2019**, *58*, 10718–10722. [CrossRef]

158. Della-Felice, F.; Sarotti, A.M.; Krische, M.J.; Pilli, R.A. Total synthesis and structural validation of phosdiecin A via asymmetric alcohol-mediated carbonyl reductive coupling. *J. Am. Chem. Soc.* **2019**, *141*, 13778–13782. [CrossRef]
159. McLafferty, F.W. *Mass Spectrometry of Organic Ions*; eBook; Academic Press: London, UK; New York, NY, USA, 1963; p. 700, ISBN 9780323142779.
160. Gerlich, D. Probing the structure of CH_5^+ ions and deuterated variants via collisions. *Phys. Chem. Chem. Phys.* **2005**, *7*, 1583–1591. [CrossRef]
161. Collins, C.J. The pinacol rearrangement. *Quart. Rev.* **1960**, *14*, 357–377. [CrossRef]
162. Dewar, M.J.S.; Rzepa, H.S. Gaseous ions. 4. MINDO-3 calculations for some simple organic cations and for their hydrogen elimination-reactions. *J. Am. Chem. Soc.* **1977**, *99*, 7432–7439. [CrossRef]
163. Lischka, H.; Köhler, H.-J. Structure and stability of carbocations $C_2H_3^+$ and $C_2H_4X^+$, X = H, F, Cl, Cl, and CH_3 –ab initio investigations including electron correlation and comparison with MINDO-3 results. *J. Am. Chem. Soc.* **1978**, *100*, 5297. [CrossRef]
164. Andrei, H.-S.; Solca, N.; Dopfer, O. IR spectrum of the ethyl cation: Evidence for the nonclassical structure. *Angew. Chem. Int. Ed.* **2008**, *47*, 395–397. [CrossRef] [PubMed]
165. Ricks, A.M.; Douberly, G.E.; Schleyer, P.v.R.; Duncan, M.A. Infrared spectroscopy of protonated ethylene: The nature of proton binding in the non-classical structure. *Chem. Phys. Lett.* **2009**, *480*, 17–20. [CrossRef]
166. Saunders, M.; Hagen, E.L. Rearrangement reactions of secondary carbonium Ions. Isopropyl cation. *J. Am. Chem. Soc.* **1968**, *90*, 6881–6882. [CrossRef]
167. Olah, G.A.; White, A.M. Stable carbonium ions. XCI: Carbon-13 nuclear magnetic resonance spectroscopy study of carbonium ions. *J. Am. Chem. Soc.* **1969**, *91*, 5801–5810. [CrossRef]
168. McAdoo, D.J.; McLafferty, F.W.; Bente, P.F., III. Ion cyclotron resonance spectroscopy in structure determination. II. Propyl ions. *J. Am. Chem Soc.* **1972**, *94*, 2027–2033. [CrossRef]
169. Chiavarino, B.; Crestoni, M.E.; Fornarini, S.; Lemaire, J.; Mac Aleese, L.; Maître, P. Infrared absorption features of gaseous isopropyl carbocations. *ChemPhysChem* **2004**, *5*, 1679–1685. [CrossRef]
170. Saunders, M.; Hagen, E.L.; Rosenfeld, J. Rearrangement reactions of secondary carbonium ions. Protonated cyclopropane intermediates formed from sec-butyl cation. *J. Am. Chem. Soc.* **1968**, *90*, 6882–6884. [CrossRef]
171. Lee, C.C.; Zohdi, H.F. Solvolytic studies with 2-methyl-[1-^{13}C]-1-propyl tosylate. *Can. J. Chem.* **1983**, *61*, 2092–2094. [CrossRef]
172. Fiaux, A.; Smith, D.L.; Futrell, J.H. Ion-molecule reaction of CH_3^+, $C_2H_5^+$, $C_3H_5^+$ and $C_3H_7^+$ with unsaturated C_2, C_3 and C_4 hydrocarbons. *Int. J. Mass Spectrom. Ion Phys.* **1977**, *25*, 281–294. [CrossRef]
173. Saunders, M.; Hagen, E.L. Rapid rearrangements in *t*-amyl cation and relative sign of coupling constants. *J. Am. Chem. Soc.* **1968**, *90*, 2436–2437. [CrossRef]
174. Saunders, M.; Budiansky, S.P. Computer modeling of multistep carbonium-ion rearrangements-Applications to methylcyclopentyl and tert-amyl. *Tetrahedron* **1979**, *35*, 929–932. [CrossRef]
175. Scholz, F.; Himmel, D.; Heinemann, F.W.; Schleyer, P.V.R.; Meyer, K.; Krossing, I. Crystal structure determination of the nonclassical 2-norbornyl cation. *Science* **2013**, *341*, 62–64. [CrossRef] [PubMed]
176. Olah, G.A.; Lukas, J. Stable carbonium ions. 54. Protonation of and hydride ion abstraction from cycloalkanes and polycycloalkanes in fluorosulfonic acid-antimony pentafluoride. *J. Am. Chem. Soc.* **1968**, *90*, 933–938. [CrossRef]
177. Olah, G.A.; Reddy, V.P.; Prakash, G.K.S. Long-lived cyclopropylcarbinyl cations. *Chem. Rev.* **1992**, *92*, 69–95. [CrossRef]
178. Mo, Y.; Schleyer, P.v.R.; Jiao, H.; Lin, Z. Quantitative evaluation of hyperconjugation in the cyclopropylcarbinyl cation and in cyclopropylborane. *Chem. Phys. Lett.* **1997**, *280*, 439–443. [CrossRef]
179. Prakash, G.K.S.; Reddy, V.P.; Rasul, G.; Casanova, J.; Olah, G.A. The search for persistent cyclobutylmethyl cations in superacidic media and observation of the cyclobutyldicyclopropylmethyl cation. *J. Am. Chem. Soc.* **1998**, *120*, 13362–13365. [CrossRef]
180. Reddy, V.P.; Rasul, G.; Prakash, G.K.S.; Olah, G.A. Structural studies of nonclassical cyclobutylmethyl cations by the ab initio method. *J. Org. Chem.* **2007**, *72*, 3076–3080. [CrossRef]
181. Franke, W.; Schwarz, H.; Thies, H.; Chandrasekhar, J.; Schleyer, P.V.R.; Hehre, W.J.; Saunders, M.; Walker, G. An experimental and theoretical-study of the degenerate carbon skeleton isomerization of the cyclopentyl cation in the gas-phase. *Angew. Chem. Int. Ed.* **1980**, *19*, 485–487. [CrossRef]
182. Franke, W.; Schwarz, H.; Thies, H.; Chandrasekhar, J.; Schleyer, P.V.R.; Hehre, W.J.; Saunders, M.; Walker, G. Entartete Isomerisierung via Kohlenstoff-Platzwechsel beim Cyclopentyl-Kation in der Gasphase. Experimenteller und theoretischer Nachweis der Existenz eines pyramidalen $C_5H_9^+$-Kations bei der unimolekularen Ethylen-Eliminierung. *Chem. Ber. Rec.* **1981**, *114*, 2808–2824. [CrossRef]
183. Franke, W.; Frenking, G.; Schwarz, H.; Wolfschütz, R. Zur Kohlenstoff-Äquilibrierung in cyclischen $C_6H_{11}^+$-Kationen in der Gasphase und zum Mechanismus der unimolekularen Ethylen-Abspaltung. *Chem. Ber. Rec.* **1981**, *114*, 3878–3895. [CrossRef]
184. Cecchi, P.; Pizzabiocca, A.; Renzi, G.; Grandinetti, F.; Sparapani, C.; Buzek, P.; Schleyer, P.V.R.; Speranza, M. Gas-phase protonation of spiropentane-A novel entry into the $C_5H_9^+$ potential-energy surface. *J. Am. Chem. Soc.* **1993**, *115*, 10338–10347. [CrossRef]
185. Szabo, K.J.; Cremer, D. Route to a kinetically stabilized protonated spirocyclopentane with a pentacoordinated carbon-atom-the missing link between bicyclo[3.2.0]hept-3-yl and 7-norbornyl cation. *J. Org. Chem.* **1995**, *60*, 2257–2259. [CrossRef]